534

US Department
of Transportation
**National Highway
Traffic Safety
Administration**

DOT HS 807 587 **May 1989**
Final Report

Simulations of Vehicle Dynamics During Rollover

The United States Government does not endorse products or manufactures. Trade or manufacturer's names appear only because they are considered essential to the object of this report.

Technical Report Documentation Page

1. Report No	2 Government Accession No	3 Recipient's Catalog No
DOT HS 807 587		

4 Title and Subtitle	5 Report Date
Simulations of Vehicle Dynamics During Rollover	May, 1989
	6 Performing Organization Code
	8 Performing Organization Report No

7 Author(s)	
Rizer, A. L., Obergefell, L. A., and Kaleps, I.	
9 Performing Organization Name and Address	10 Work Unit No (TRAIS)
Armstrong Aerospace Medical Research Laboratory	11 Contract or Grant No
Wright-Patterson AFB, OH 45433-6573	13 Type of Report and Period Covered
12 Sponsoring Agency Name and Address	Final October 1986 - May 1989
U. S. Dept. of Transportation Portation National Highway Traffic Safety Administration 400 7th Street, S.W. Washington, DC 20590	14 Sponsoring Agency Code

15 Supplementary Notes

16 Abstract

The capability to predictively simulate vehicle rollover dynamics using the Articulated Total Body (ATB) model was developed and validated using the results of two controlled automobile rollover crash tests. The vehicle was modeled as a single rigid body with vehicle contact surfaces approximated by (hyper)ellipsoids. Appropriate vehicle mass, center of mass, rotational inertial properties, initial conditions, and the interactive geometry between the vehicle and the crash environment were specified. The events simulated were a multiple crash/rollover in which a vehicle was induced to roll by a ramped guardrail and a rollover which was initiated by an active rollover test device developed by the National Highway Traffic Safety Administration. The results of these computer simulations were compared with high-speed film coverage of the tests using computer graphics images of the predicted vehicle positions. Also compared were the linear and angular accelerations, velocities, displacements, and kinetic energies. The simulated results compared well to the test results. Particularly good agreement was achieved for vehicle position in time. Angular velocities also showed good agreement. Poorest agreement was between the simulated and measured vehicle accelerations.

17 Key Words	18 Distribution Statement
Rollover, Crash Testing, Vehicle Dynamics	Document is available to the public from the National Technical Information Service, Springfield, VA 22161

19 Security Classif (of this report)	20 Security Classif (of this page)	21. No of Pages	22 Price
Unclassified	Unclassified		

Form DOT F 1700.7 (8-72) Reproduction of completed page authorized

TABLE OF CONTENTS

INTRODUCTION

The most common injury-causing motor vehicle crashes involve major impacts to the vehicle's front or side. Consequently, substantial research has been focused on efforts to better understand and reduce the injury potential of such crashes. Safety improvements include better passenger compartment integrity, more benign interior contact surfaces, and improved restraint systems, including ones with airbags. Less attention has been given to the injury potential of vehicle rollover and to the design of restraint and containment systems which minimize the injury potential in rollovers. The present effort studies rollover crashes in order to determine how best to provide improved rollover crash protection.

Two methods of studying vehicle crashes are available: extensive and costly full-scale testing and computer simulation. Full-scale crash testing is necessary and desirable. However, considerable insight and design guidance can be obtained fron predictive analytical models. The most ideal approach employs both these methods. Full-scale testing provides baseline data which are used to validate computer simulations. Validated simulations can then be used for initial test design, evaluation of test condition variations, the investigation of vehicle design changes to minimize occupant injuries, and the study of specific rollover

crashes that are not experimentally feasible. The investigation of occupant injuries in rollover tends to fall in the latter category.

While full-scale rollover crash tests have been performed in recent years, the primary vehicle motion in these tests has been a simple longitudinal roll. While this mode of testing may help to evaluate a vehicle's resistance to roof crush and the violence of an occupant's motion, it does not adequately represent the full spectrum of dynamic responses that vehicles experience in rollover crashes. Addressing this spectrum of responses in a testing program is difficult for two reasons: 1) A very large number of tests would have to be conducted; and 2) one cannot specify with consistency prior to the test the motion of the vehicle. It is specifically in the area of repeatability, which is essential to evaluate methods to minimize injury, that computer simulation has many of its advantages. The vehicle motion can be exactly specified and is xactly repeatable. Thus, computer simulation is excellent for performing studies in which only one factor is varied at a time. Such a study would be virtually impossible with full-scale testing using dummies. In addition, the cost of computer simulation is generally much less than that of full-scale crash testing. Of course, to be totally confident in the results of computer simulation, some parallel crash testing must be done to verify the accuracy of the prediction of both the vehicle and the occupant motion.

This effort describes the application of a coupled rigid body dynamics program in order to predict the motion of the vehicles themselves for two separate rollover crash tests. The simulations are of actual test events and results of the simulations are compared to those of the tests. Predictions of the dummy motions for these two tests have already been reported in References 3 and 4.

BACKGROUND

In the early 1970's, the National Highway Traffic Safety Administration contracted with Calspan Corporation to develop a computer program which predicts the dynamics of an occupant during a vehicle crash. This program was called the Crash Victim Simulator (CVS) [Ref. 1]. The Harry G. Armstrong Aerospace Medical Research Laboratory at Wright-Patterson Air Force Base applied this program to predict the motion of humans and manikins in various dynamic environments, including ejection from aircraft and windblast, as well as automobile crashes. A number of modifications were made to the CVS to better address Air Force problems and the resulting program was renamed the Articulated Total Body (ATB) model [Ref. 2].

Before the ATB model could be used for parametric studies of occupant motion during rollover, it was necessary to verify that the ATB is capable of accurately predicting occupant motion during the prolonged and complex motion of a rollover

crash. For this purpose, a number of controlled, fully-instrumented rollover crash tests were conducted and the motion of the dummy occupants were predictively simulated with the ATB model [Ref. 3 and 4]. These tests were filmed with high-speed cameras located at various points external to the vehicles and also with cameras inside the vehicles focused on the occupant motion. In each test, the vehicle's motion, as recorded by high-speed cameras mounted at various points on the ground, was digitized and analyzed to provide reconstructed vehicle motion, required as input by the ATB model. The other test conditions, including the properties of the dummy, internal vehicle contact geometry, and restraint system, were specified in the model and the simulations were conducted. A few adjustments in the input prescription were necessary in order to get good agreement between the predicted and observed dummy motion because some of the data were initially estimated. From these simulations of actual rollover crash tests, modified simulations could be conducted in which some of the test conditions were varied. These could include restraint system or interior structure modifications of the vehicle, changes in the vehicle motion, or the use of different sized occupants in different initial positions. A series of these predictive simulations, constituting a parametric study, could be useful in determining how best to protect an occupant during rollover crashes.

Parametric studies similar to these have been performed and have proven quite useful [Ref. 5]. There are, however, two constraining factors in this process: (1) an actual vehicle crash test must first be performed, and (2) the film of the resulting vehicle motion must then be analyzed. In order to realize the full advantages of computer simulation, one should have the capability to predict occupant motion during any crash initiated by specified means, whether it is a fully instrumented crash test, a real-world crash, or a purely hypothetical one. One way to accomplish this would be to use the ATB model to predict the vehicle motion, using the initial vehicle conditions at roll initiation and a prescription of the physical environment that interacts with the vehicle during the rollover. This predicted vehicle motion would, in turn, be used to prescribe the vehicle motion for the occupant simulation. This process greatly reduces both time and costs even when crash tests are available, because the film analyzing process for vehicle motion reconstruction, which is highly time-consuming, is avoided.

The objective of this study was to develop the methodology required, using the ATB model, to accurately predict the crash/rollover motion of a vehicle given the set of vehicle conditions at rollover initiation and a prescription of the forces exerted on the vehicle by the crash environment. With

the methodology adequately developed, accident investigators could use the process on a trial and error basis to reconstruct rollover crashes.

In order to verify the validity of this methodology, the initial conditions of two actual tests were used as input specifications for the model and two simulations were made. The first test consisted of rolling a 1981 Plymouth Reliant off a rollover test device and the second consisted of impacting the end of a turned-down guardrail with a 1982 Dodge Aries. Since these two car models have such similar body properties, they were modeled using the same set of body specifications. The predicted motions were compared with the motions of the actual test vehicles using visual comparisons of the vehicles and graphical plots of kinematic data.

DESCRIPTION OF ATB MODEL

The Articulated Total Body Model is an analytical program based on coupled rigid-body dynamics methods using Euler equations of motion with Lagrange type constraints. Although this model was originally developed to study human body and anthropomorphic dummy dynamics during automobile crashes, its flexible structure enables the modeling of much more diverse systems. The input to the model defines the specifics of the system. These systems are described as sets of rigid segments that are connected by joints. These joints allow the transfer of

moments and forces due to constraints, as well as torques as functions of joint orientation, between the segments. The outer surfaces of the segments are defined by contact (hyper)ellipsoids that are rigidly attached to the segments. Each segment may have more than one contact (hyper)ellipsoid associated with it. The magnitudes and points of application of external forces, such as those caused by interactions with other segments, planes, and belt restraint systems are dependent upon the geometry of the contact (hyper)ellipsoids. The ATB model also requires functions which relate: the magnitudes of the contact forces to the amount of mutual deflection of the contact surfaces, the magnitudes of the joint torques to the rotation angles, and the magnitudes of belt, wind, and spring forces to other appropriate parameters.

In this study, the vehicle was modeled as a single rigid segment with a number of contact (hyper)ellipsoids rigidly attached to it. The geometries and locations of these (hyper)ellipsoids were chosen to provide appropriate ground-vehicle contacts based upon the actual dimensions of the vehicle. Since only one segment was used for the car, no joints were needed and, due to the specific application, no harness system or wind forces were used.

ROLLOVER DEVICE CRASH TEST

DESCRIPTION OF TEST

The first test analyzed to simulate vehicle rollover dynamics was one of a series of rollover crash tests conducted by the Transportation Research Center of Ohio for the National Highway Traffic Safety Administration. In this test, rollover was initiated in a 1981 Plymouth Reliant 4-door by a rollover test device (RTD), shown in Figure 1 [Ref. 6 and 7]. This particular set-up was chosen for the first simulation because of its relative simplicity and the abundance of data available.

The RTD was designed so that the initial orientation of the vehicle can be varied. The wheels of the RTD are allowed to rotate about a vertical axis so that the device, along with the car placed on top of it, can be crabbed at an initial yaw angle (Figure 2). The actuating cylinders cause the platform on which the test vehicle is mounted to rotate about a horizontal axis. To give the vehicle an initial linear velocity, a cable tows the RTD along a guiderail at the desired velocity. At a specified point along the guiderail, the cylinders actuate, causing angular acceleration of the platform and giving the platform and car an initial roll velocity. Finally, the test vehicle separates from the platform, and the RTD is rapidly decelerated to a stop so that it does not run into the test

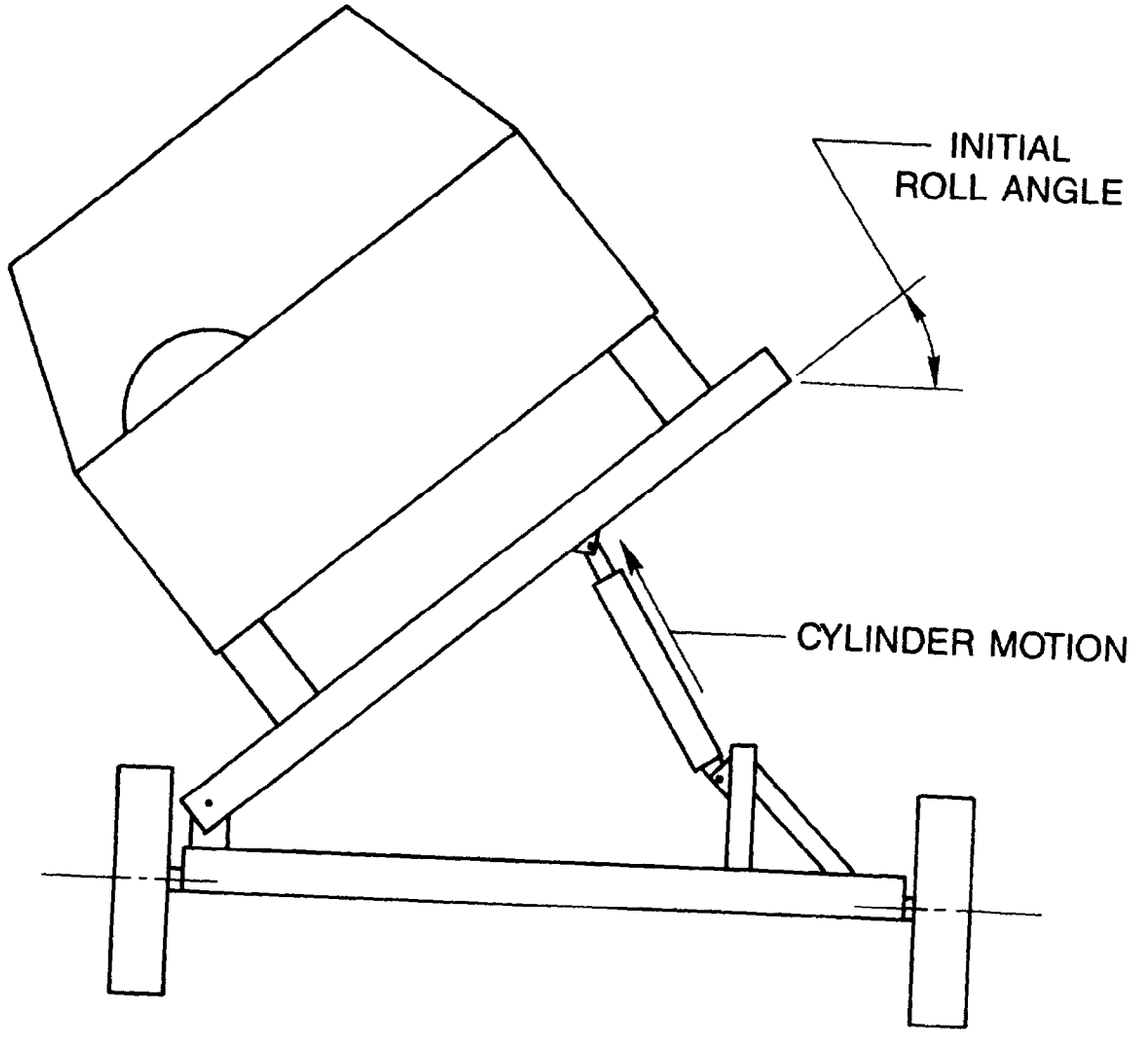

Figure 1 Rollover Test Device (RTD)

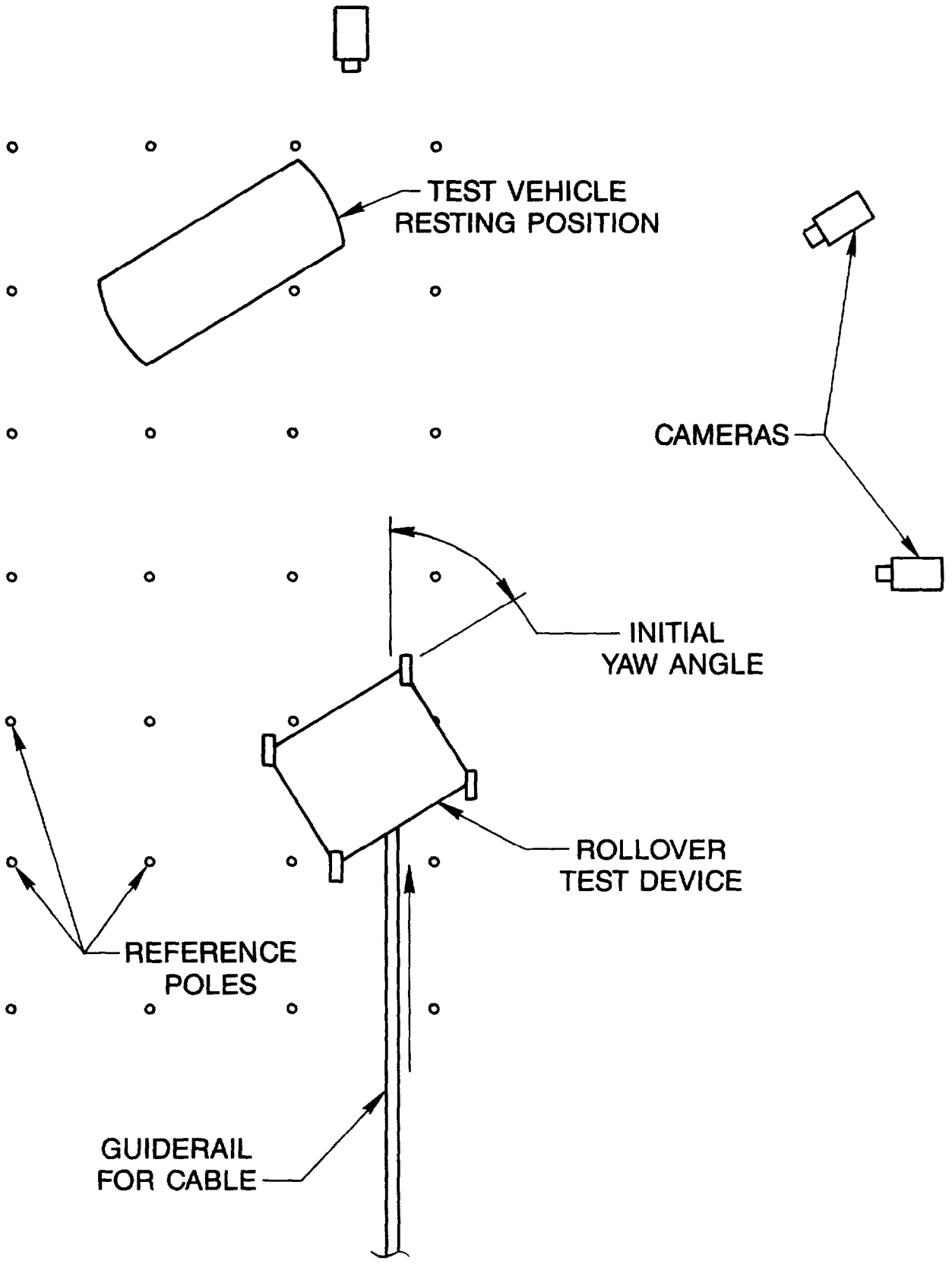

Figure 2 Layout of Rollover Device Crash Test

vehicle. For this particular test, the initial orientation was 42 degrees yaw and the initial linear velocity at separation from the RTD was 21 mph.

The layout of the test area is shown in Figure 2. Breakaway poles were placed on the ground as reference points for cameras, which were located at various points on the ground and filmed the vehicle motion for future comparison to simulated motion. After the vehicle separated from the RTD, it rolled one and one-half times and came to rest on its roof.

VEHICLE MODEL

The ATB program requires that the surface of the test vehicle be modeled with ellipsoids. For this particular rollover crash, it was decided that eight ellipsoids, rigidly attached to a single segment, would adequately represent the vehicle's various deformable surfaces. These eight ellipsoids represented the four tires, the front and rear bumpers, and the front and rear windshield/roof surfaces [Fig. 3]. When the hyperellipsoid option of the ATB program recently became available, the front and rear bumper surfaces were changed to hyperellipsoids to better model the blockish shape of these parts. The dimensions of the car were obtained from the Motor Vehicle Manufacturers' Association Specifications on a 1981 Dodge Aries [Ref. 8]. The size, shape, and location of the ellipsoids were based upon these dimensions.

VEHICLE CONTACT SEGMENTS/ELLIPSOIDS

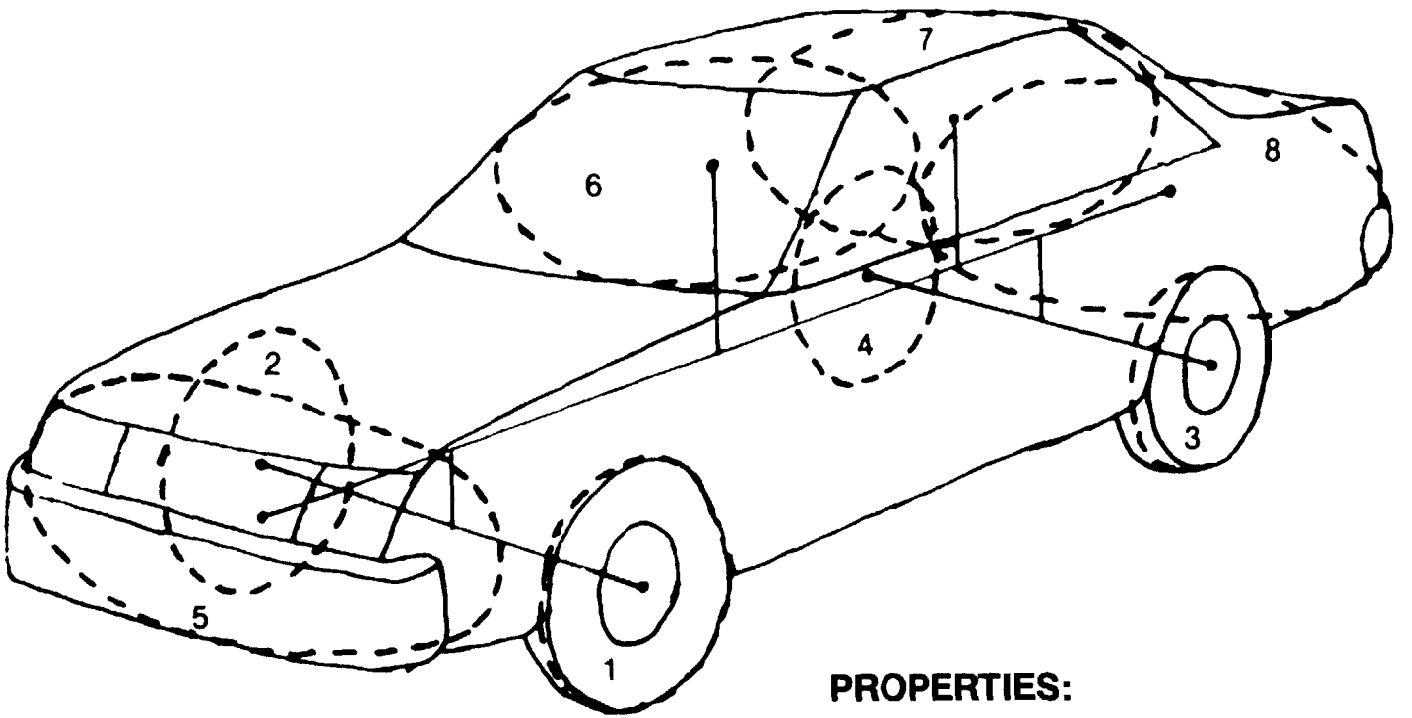

		PROPERTIES:
		CENTER OF MASS
1–4	WHEELS	MASS
5	FRONT BUMPER	MOMENTS OF INERTIA
6	FRONT ROOF	CONTACT ELLIPSOID PLACEMENT/GEOMETRY
7	REAR ROOF	CONTACT SEGMENT JOINT CHARACTERISTICS
8	REAR BUMPER	CONTACT FORCE-DEFLECTION CHARACTERISTICS

Figure 3 Vehicle Contact Ellipsoids

The inertial properties of the vehicle were taken from a variety of sources. The mass and the center of gravity of the vehicle, with the manikin and instrumentation in place, were measured at the test site before the rollover was performed. The moments of inertia were more difficult to obtain. Measured values of the moments of inertia for this car model were not available, so an estimation had to be made based upon data taken from a number of older model cars [Ref. 9]. Data from the most similar of these cars was scaled down to fit the test vehicle, using the dimensions and masses of the test vehicle and the other cars as scale factors.

The force-deflection and friction characteristics for the vehicle-ground contacts were estimated. The force-deflection characteristics were defined in terms of a force-deflection function, an energy absorption function, and a permanent deflection function. These functions were adjusted as the preliminary simulations were performed and analyzed so that the simulated vehicle motion better matched the actual vehicle motion.

INITIAL CONDITIONS

For these simulations, two orthogonal axes systems are defined: the inertial coordinate system and the vehicle coordinate system. The origin of the inertial coordinate system is located at the point on the guiderail where rollover was

initiated. The X axis is parallel to the guiderail that the vehicle was towed along and is in the direction of vehicle motion, the Y axis is directed from left to right, and the Z axis is directed toward the ground. The vehicle coordinate system is attached to the vehicle with its origin at the center of gravity, the X axis directed from the rear to the front of the vehicle, the Y axis directed from left to right, and the Z axis directed from top to bottom of the vehicle. All quantities of linear motion and angular displacement are given in the inertial coordinate system and angular velocity is given in the vehicle coordinate system.

The initial conditions of the vehicle used as input to the ATB were those kinematic values existing when the vehicle completely separated from the RTD, occurring 885 msec after time zero of the crash test. These kinematic values (linear and angular velocities and displacements) were obtained by analysis of vehicle motion film data, performed for the earlier study [Ref. 4]. The values for these initial kinematic parameters are as follows:

	X	Y	Z
Linear Velocity (in/sec)	376.296	-58.851	165.737
	X	Y	Z
Linear Displacement (in)	279.442	-31.075	-50.269
	X	Y	Z
Angular Velocity (deg/sec)	-115.930	-60.807	12.395
	Yaw	Pitch	Roll
Angular Displacement (deg)	47.890	-6.890	-77.400

SIMULATION RESULTS

The results of the vehicle simulation are given in two formats: (1) Comparisons of the film images with computer-generated images of the ATB simulation, and (2) plots of kinematic and dynamic values for the test and the simulation. The "test" data shown in the plots are actually reconstructed values from the film analysis phase of the previous study.

VIEW Graphics

The vehicle motion during this crash test was recorded at high-speed (500 fps) on film by several ground based cameras located in the test area. One of these views, showing the motion throughout the majority of the test, was chosen to evaluate the vehicle simulation. The VIEW computer graphics program [Ref. 10] was used to generate three-dimensional images of the motion of the vehicle as predicted by the ATB simulation. The VIEW images were generated with respect to the same viewing angle as that of the chosen camera so that a direct comparison can be made between the predicted and the actual motions.

Figure 4 shows the film images and the simulated images of the vehicle motion starting at time zero, which is defined as the moment after the vehicle separates from the test device, and proceeding at 200 msec intervals. The motion matches quite well for the first 800 msec. At 1000 msec, the simulated

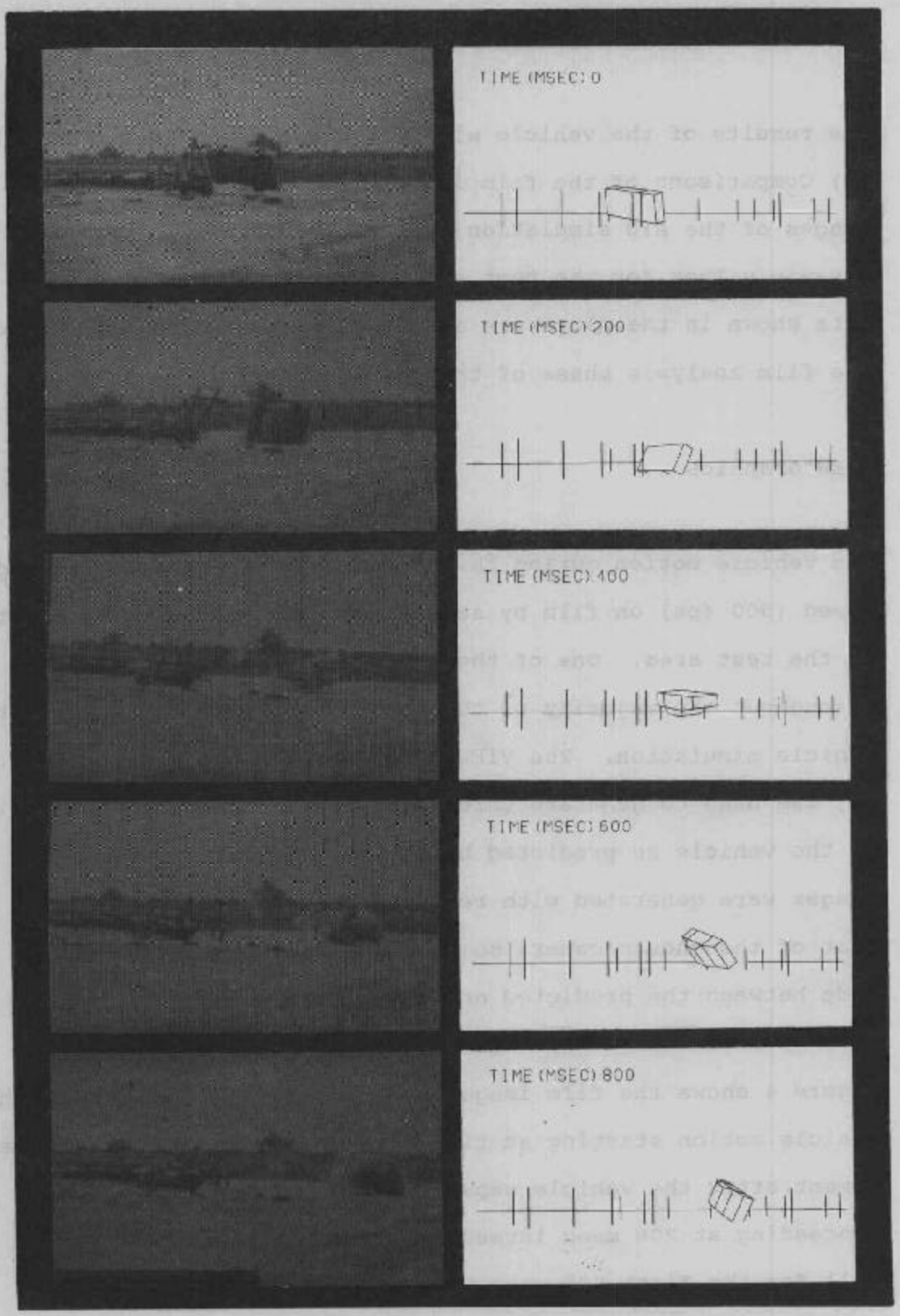

Figure 4 Rollover Device Crash Test
Test Film and Simulated Motion

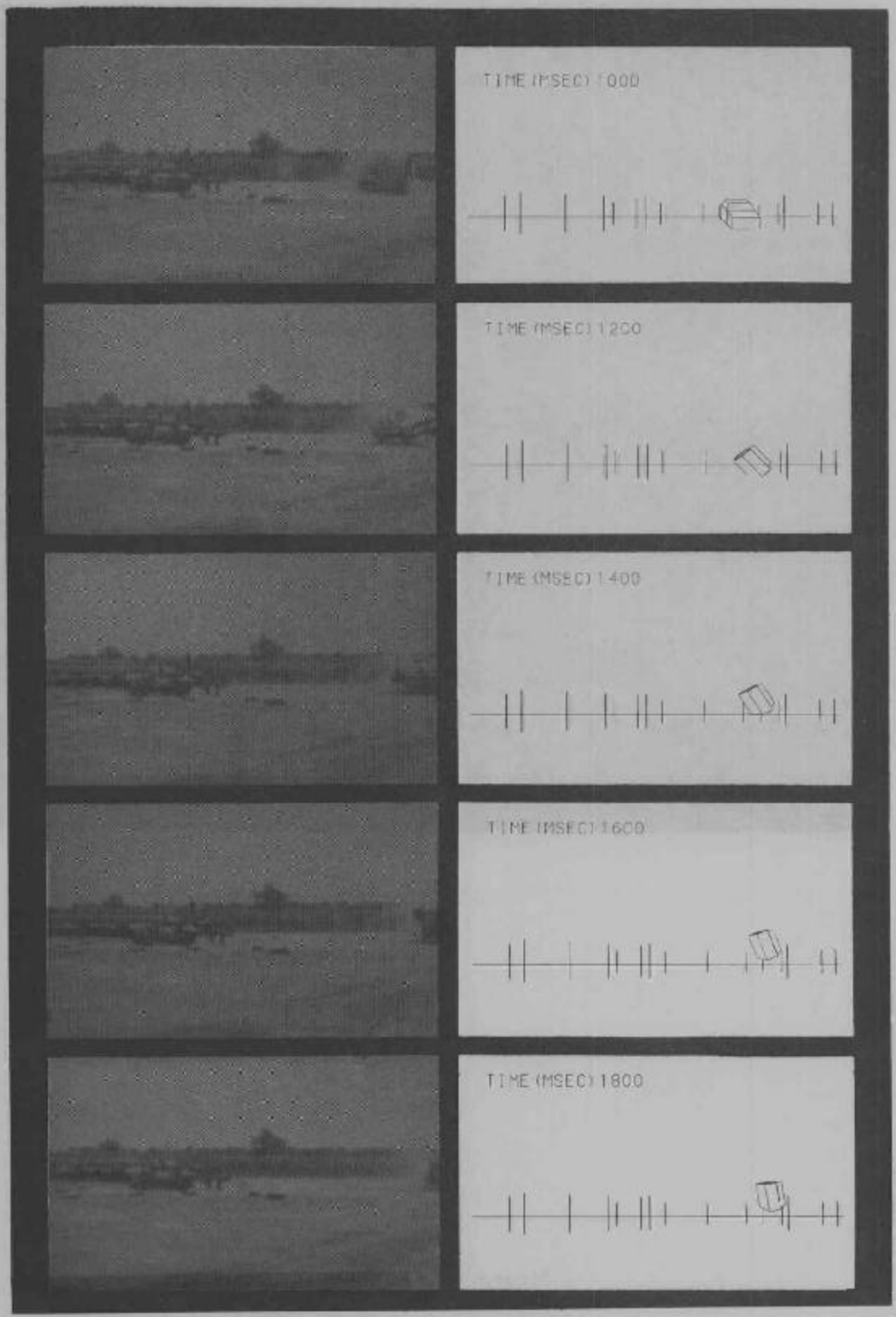

Figure 4 continued

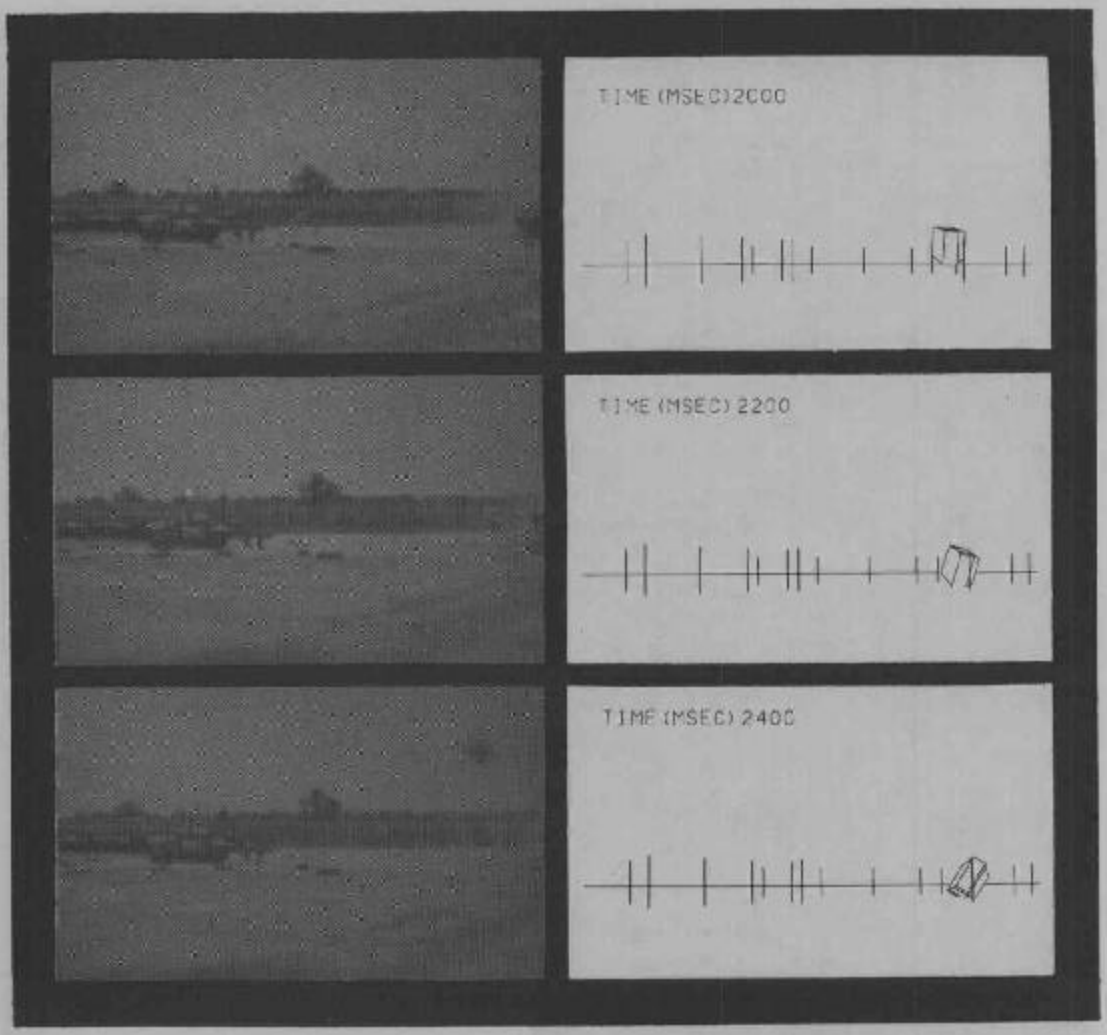

Figure 4 continued

vehicle has rolled approximately 60 degrees more than the actual vehicle and this difference is maintained through 1200 msec. At 1400 msec, the orientations again become more closely aligned and by 1600 msec, they are almost identical.

The actual vehicle continues to roll more rapidly than the simulated vehicle until about 2400 msec when its rolling motion stops. The simulated vehicle, while rolling at a slower rate during this period, continues to roll beyond 2400 msec and does not stop rolling even at 4000 msec when the simulation is terminated.

While the initial conditions and actual motion match well between the actual test and the simulation through about 800 msec, the motion beyond 800 msec was not a good match. The primary reason was the inability to absorb sufficient energy in the simulation. This resulted in excessive bouncing in which the vehicle was totally off the ground, which did not occur in the actual test. During these periods, surface frictional forces did not act to modify the rolling rate. Additionally, standard ellipsoids were used for the roof contact surface and these, because of their rounded contours, did not produce as large a resistance to rolling as were experienced by the actual vehicle.

Data Time Histories

The ATB model calculates various kinematic values which can be plotted as a function of time to compare to the corresponding measured values. In this section, the data generated during the vehicle simulation are compared to the data obtained during the analysis of the films of the vehicle motion, hereafter referred to as the "reconstructed motion data". The reconstructed motion data are assumed to be accurate in describing the actual motion of the vehicle.

Since the intent of the predictive simulation of the vehicle dynamics was to match the simulated motion against the reconstructed motion data, all linear acceleration, velocity, and displacement variables were converted to the inertial coordinate system. While a comparison in the inertial system facilitated the development of the predictive simulation method, it precluded a possible comparison between vehicle on-board accelerometer measurements and the predicted results.

The primary objective in this study was to adjust vehicle and ground contact properties to best match vehicle position and kinetic energy over time for the simulated and reconstructed events. The best matches that were obtained are shown in Figures 5 through 10. Figure 5 shows the relatively poor agreement of the respective linear accelerations. The two main reasons for this were 1) the reconstructed motion had been

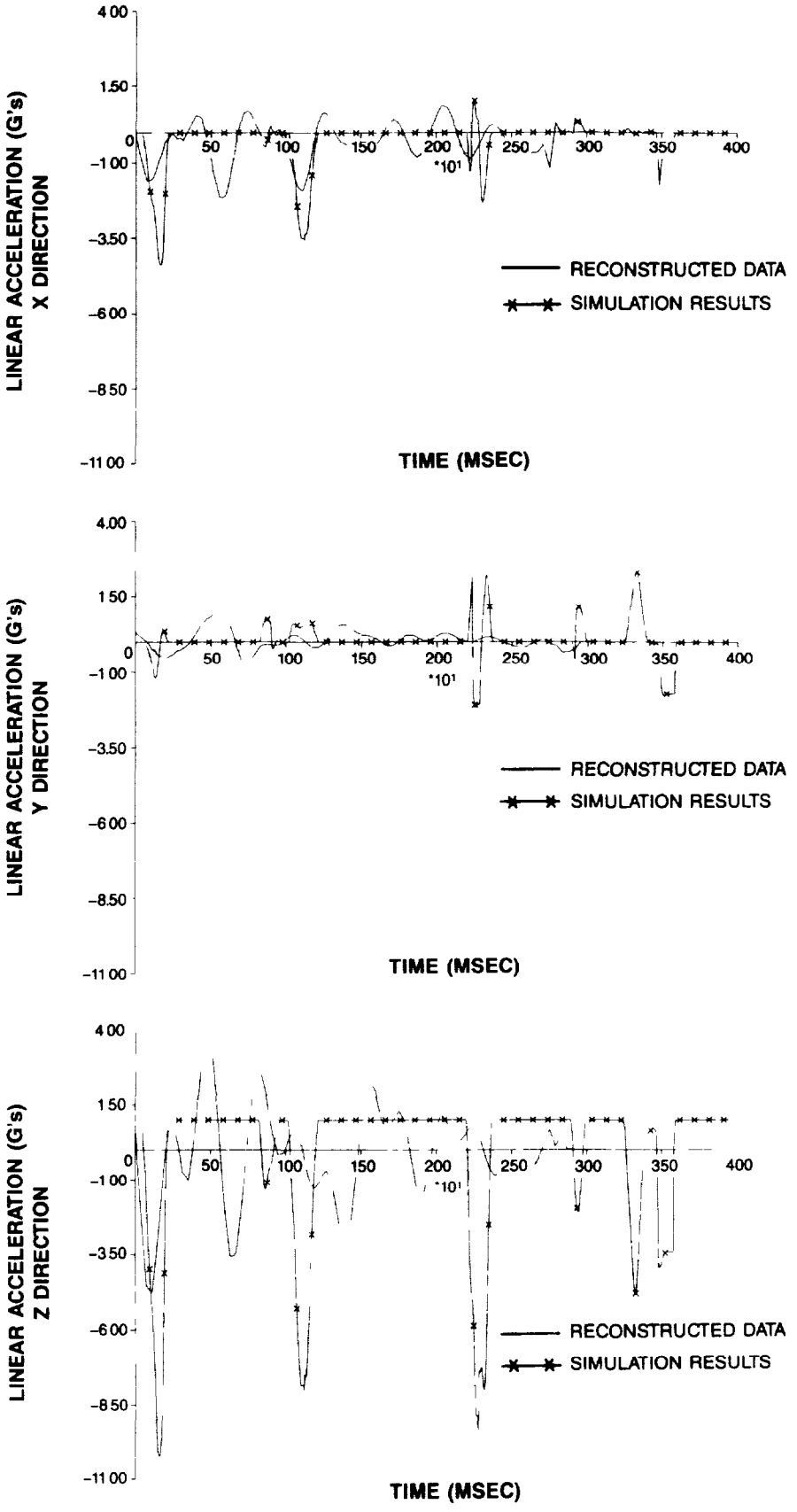

Figure 5 Reconstructed and Simulated Linear Accelerations

obtained using position data which had subsequently been filtered to reduce noise introduced in differentiating the data, and 2) the ATB model was unable to analytically extract adequate energy during the ground impacts. The first factor contributed to lower acceleration peaks in the reconstructed data than what was predicted. The second factor did not allow sufficiently rapid energy absorption during rolling, resulting in time-shifted acceleration peaks, too large peaks during the latter part of the roll motion, and continued vehicle motion beyond the reconstructed motion vehicle stop time. The periods of constant Z axis acceleration represent vehicle acceleration while off the ground. Physically, this type of response is reasonable, though the length of time that the vehicle is airborne may be accentuated due to the model's inability to absorb sufficient energy during ground contacts. The lack of constant acceleration periods in the reconstructed data further demonstrates the problem of deriving accelerations from position measurements.

The linear velocities [Figure 6], on the other hand, match fairly well in the magnitudes and the general trends, although the timing of the peaks and valleys does not match well. These plots also indicate the intervals in which gravity was the only force acting on the vehicle. In the inertial X and Y directions, these intervals are characterized by periods of constant velocity equal to the velocity of the vehicle when it left the ground. In the Z direction, the curve has a constant

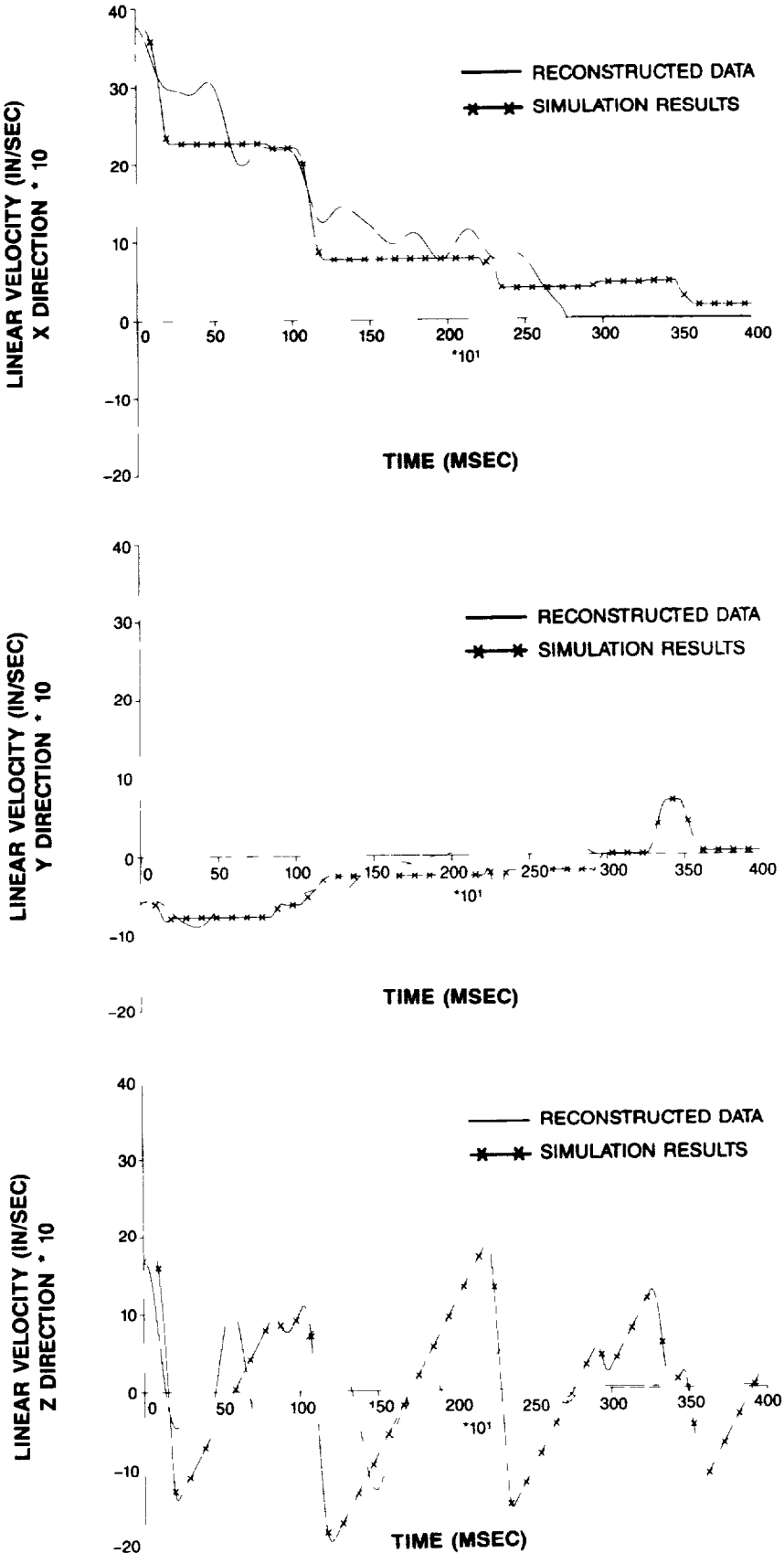

Figure 6 Reconstructed and Simulated Linear Velocities

positive slope during these periods. Figure 7 shows the linear displacements. These match better than the velocities, particularly in the X direction. It is evident from the plot of the Z component of linear displacement that the simulated car consistently bounces higher than the car in the actual test. This indicates a problem with absorbing kinetic energy, which will be illustrated further in the kinetic energy plots.

The angular velocities are given in the vehicle coordinate system and the angular displacements are given in the inertial coordinate system. Figure 8 shows the angular velocity plots and Figure 9 the angular displacement plots. These all match fairly well. The most obvious differences in the velocity plots are that the simulated motion has almost constant plateaus whereas the reconstructed motion data does not. These plateaus are due to the lack of an applied torque to the simulated vehicle when it is airborne.

The kinetic energy plots are displayed in Fig. 10. These clearly show that less energy was absorbed in the predictive simulation than observed from motion reconstruction. Note that the amount of kinetic energy due to angular motion is almost an order of magnitude less than that due to linear motion.

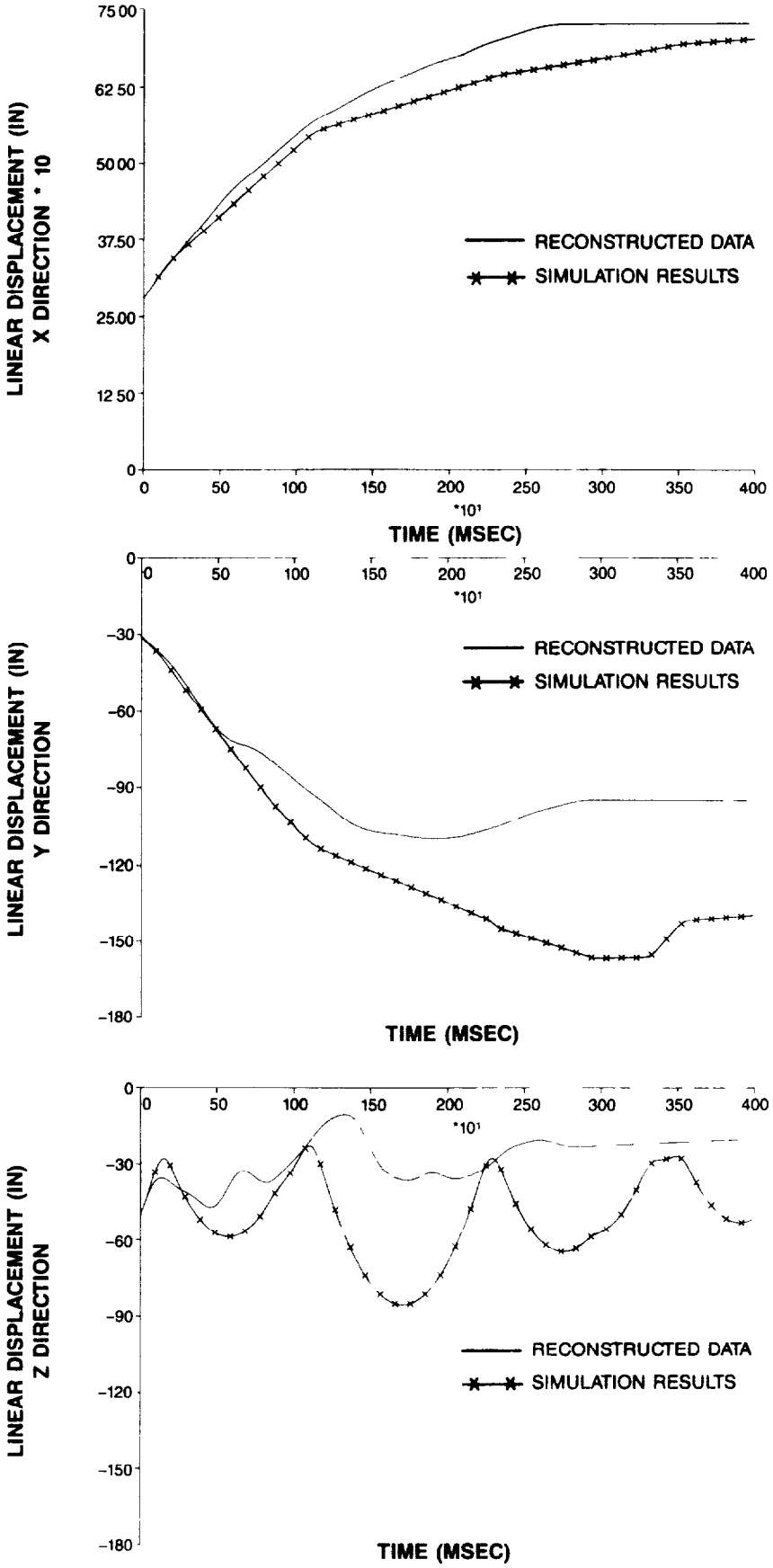

Figure 7 Reconstructed and Simulated Linear Displacements

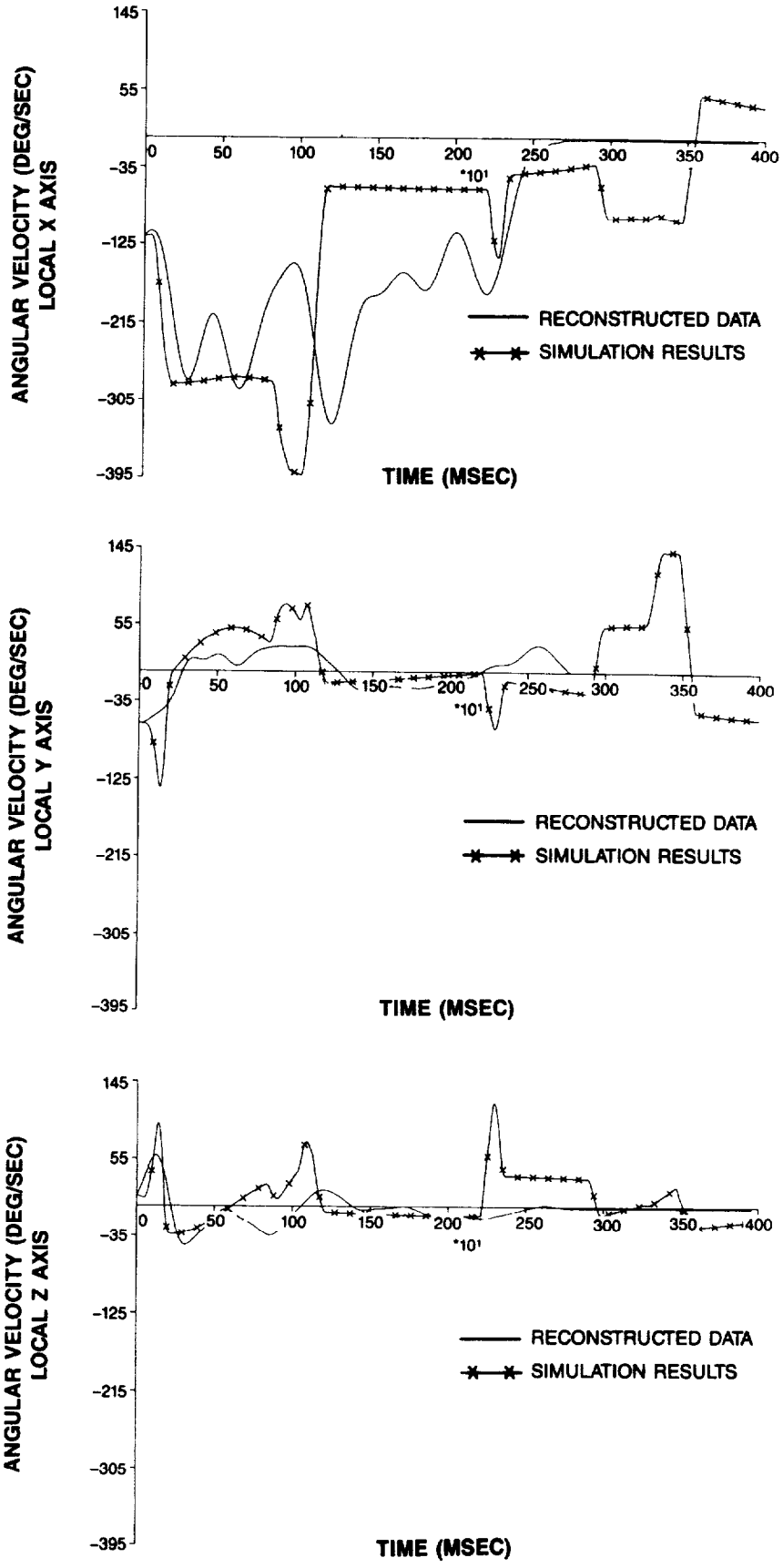

Figure 8 Reconstructed and Simulated Angular Velocities

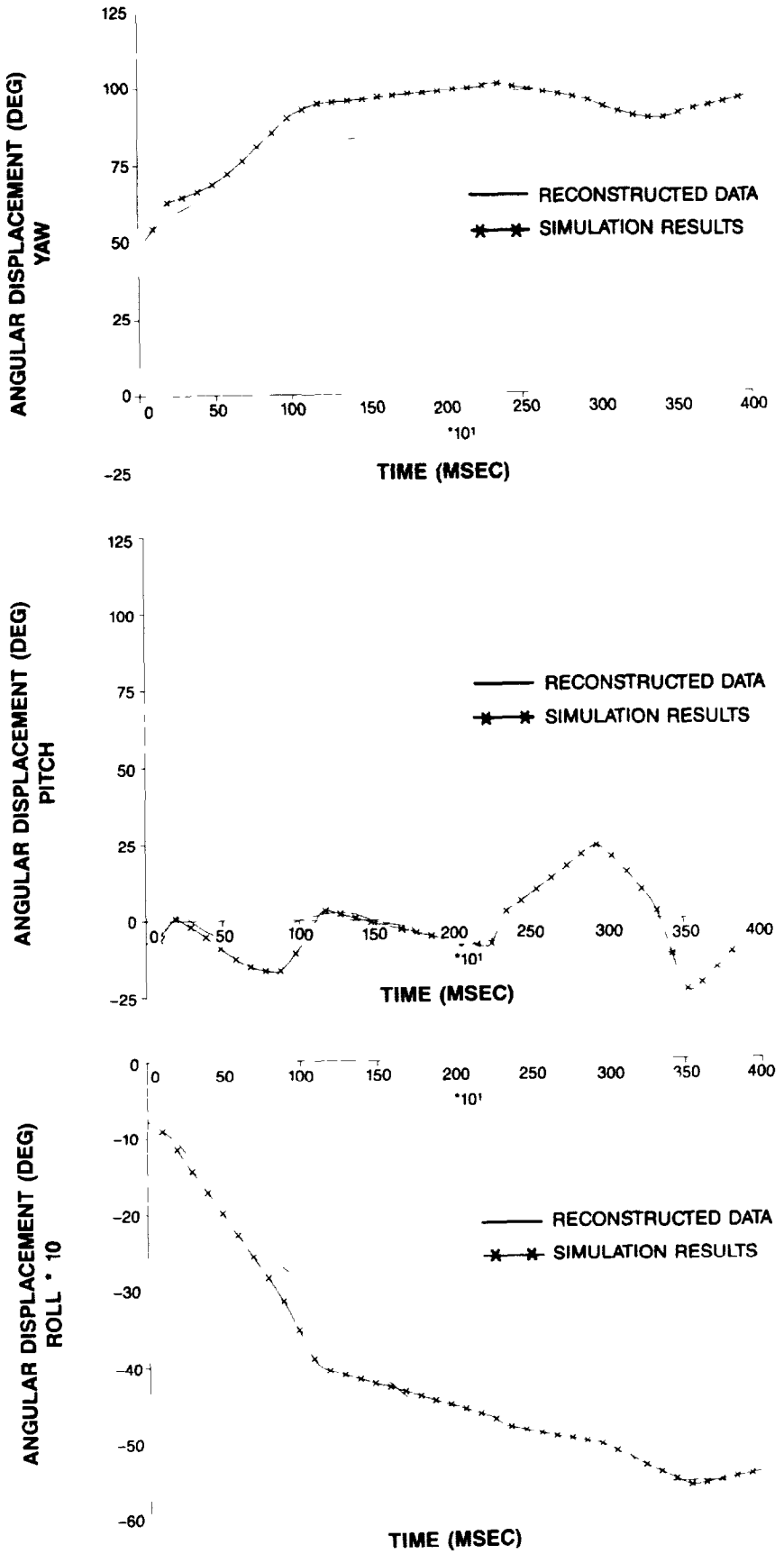

Figure 9 Reconstructed and Simulated Angular Displacements

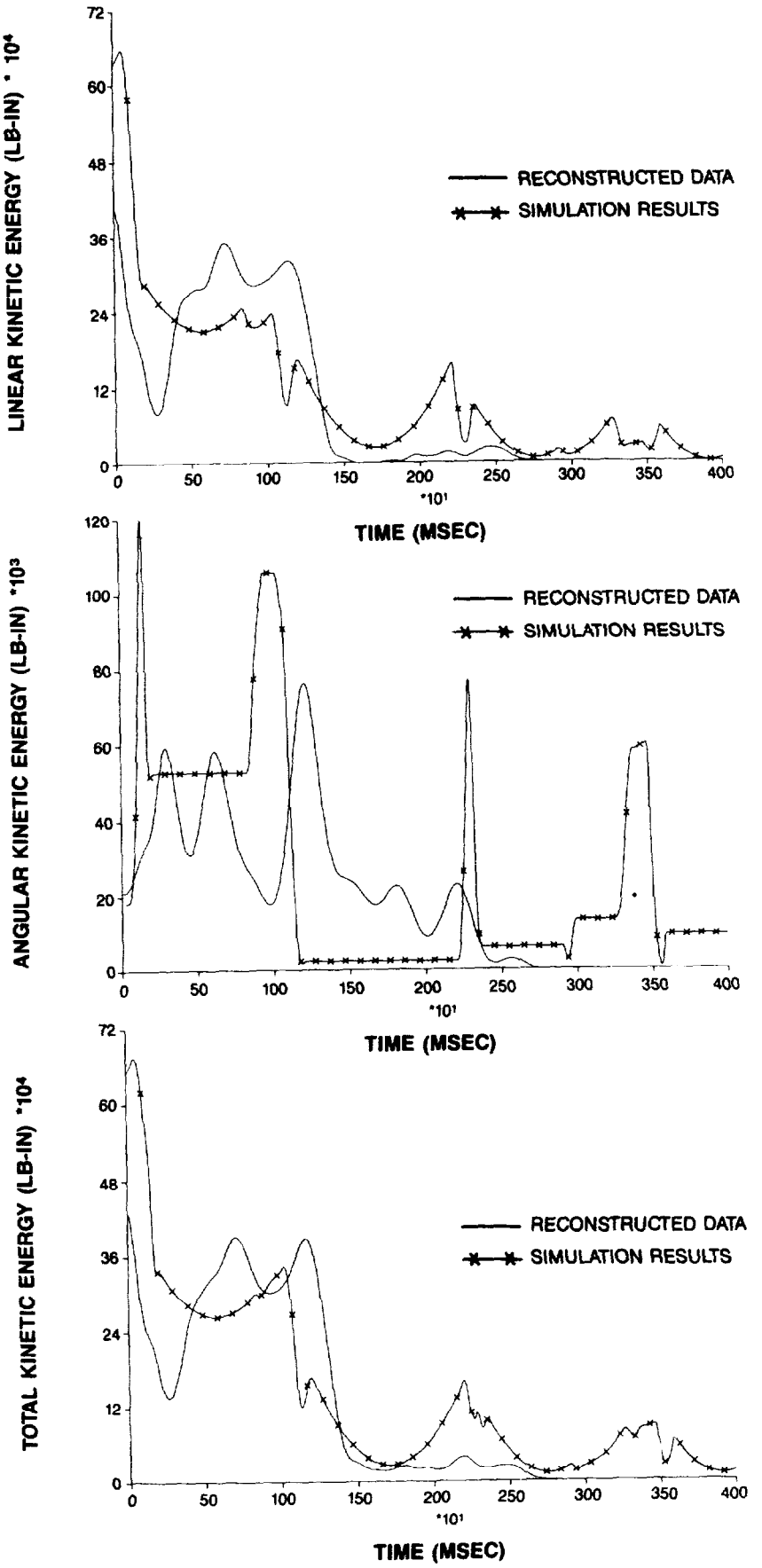

Figure 10 Reconstructed and Simulated Kinetic Energies

PARAMETRIC STUDIES

One difficulty in performing these types of vehicle simulations is the lack of data on certain characteristics of the vehicles that are needed for the dynamics simulation. This is particularly true for the moments of inertia and the contact force deflection characteristics. For these simulations, these data were initially estimated and then, by analyzing the preliminary simulations, adjusted as required within physically reasonable limits to improve the predictions. The effects of varying 1) the moment of inertia of the vehicle about its X axis and 2) the friction coefficient between the vehicle and the ground on the vehicle's motion were examined.

Effects of X Moment of Inertia Variation

In the rollover crash test simulation described above (the "baseline simulation"), the value of the X moment of inertia (Ixx) was 3897 in-lb-sec**2. To examine the sensitivity to changes in Ixx, simulations were performed with 80%, 90%, 110%, and 120% of the baseline Ixx value. All other input parameters were unchanged. The resulting VIEW plots from these simulations, compared to the baseline simulation, are shown in Figure 11. The motions are very similar for the first 800 msec. At 1200 msec, the positions begin to significantly diverge. For reduced Ixx moments, the initial roll rate is greater than for the baseline case and for increased Ixx

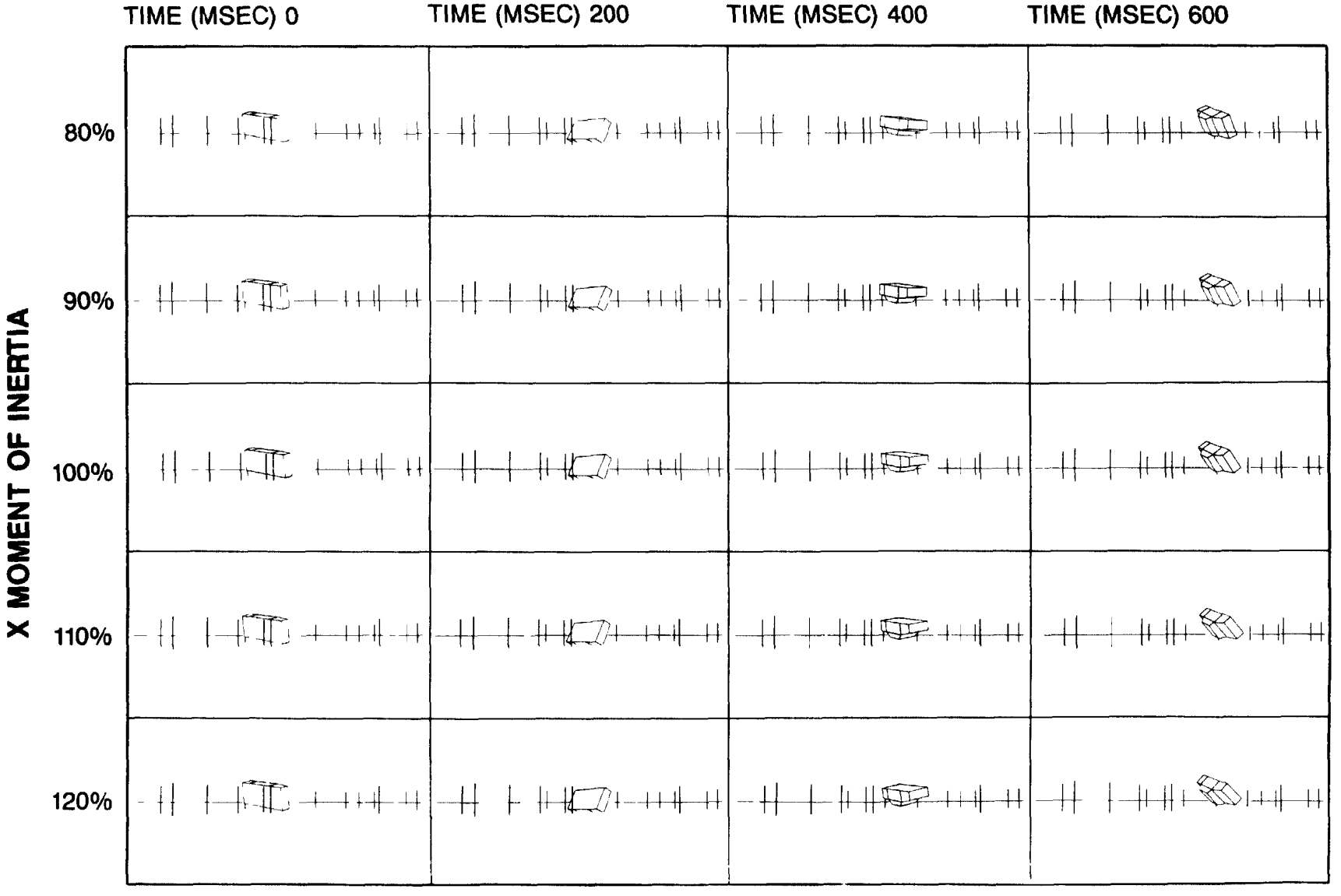

Figure 11 X Moment of Inertia Parameter Study
Vehicle Motion

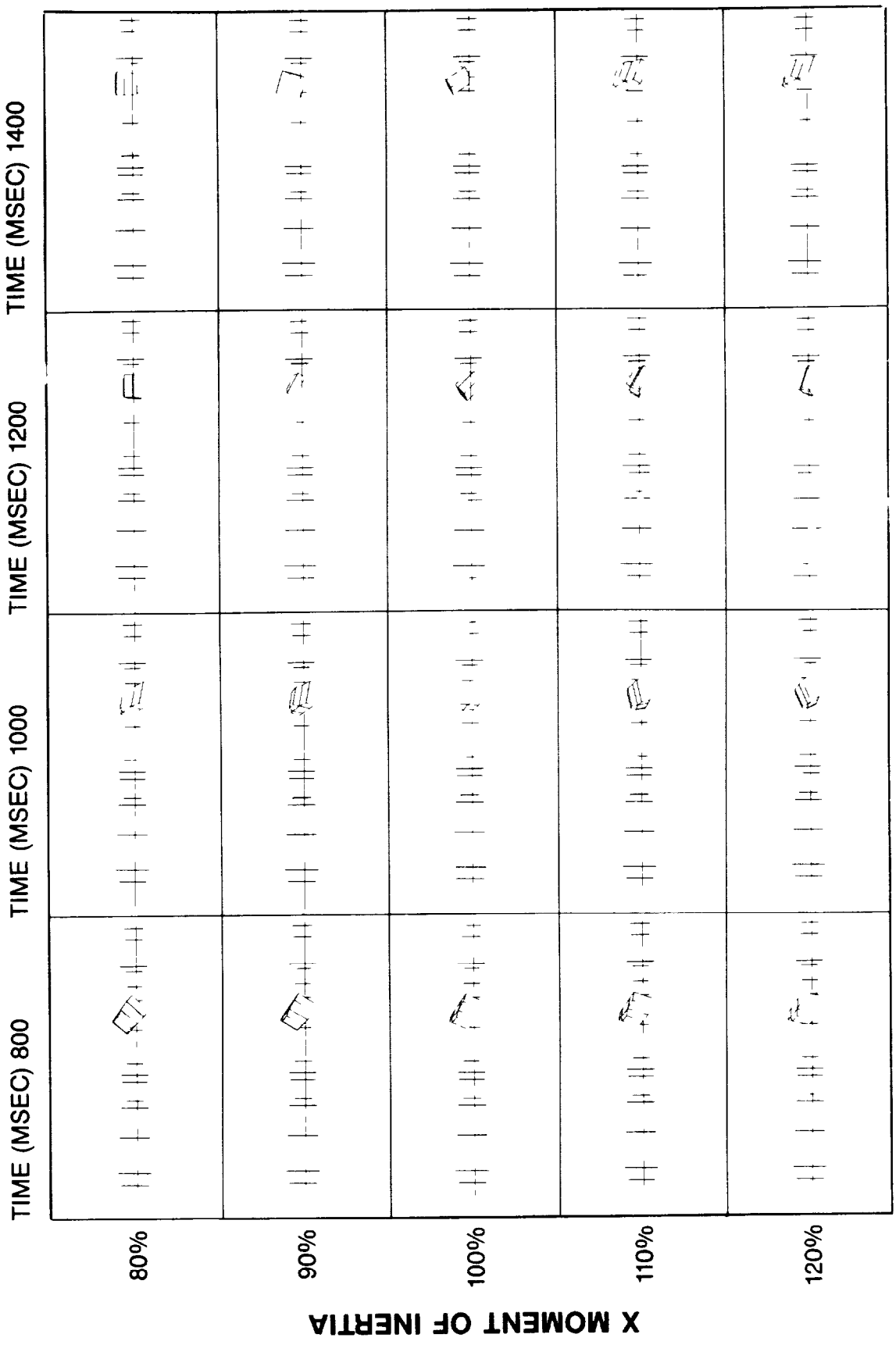

Figure 11 continued

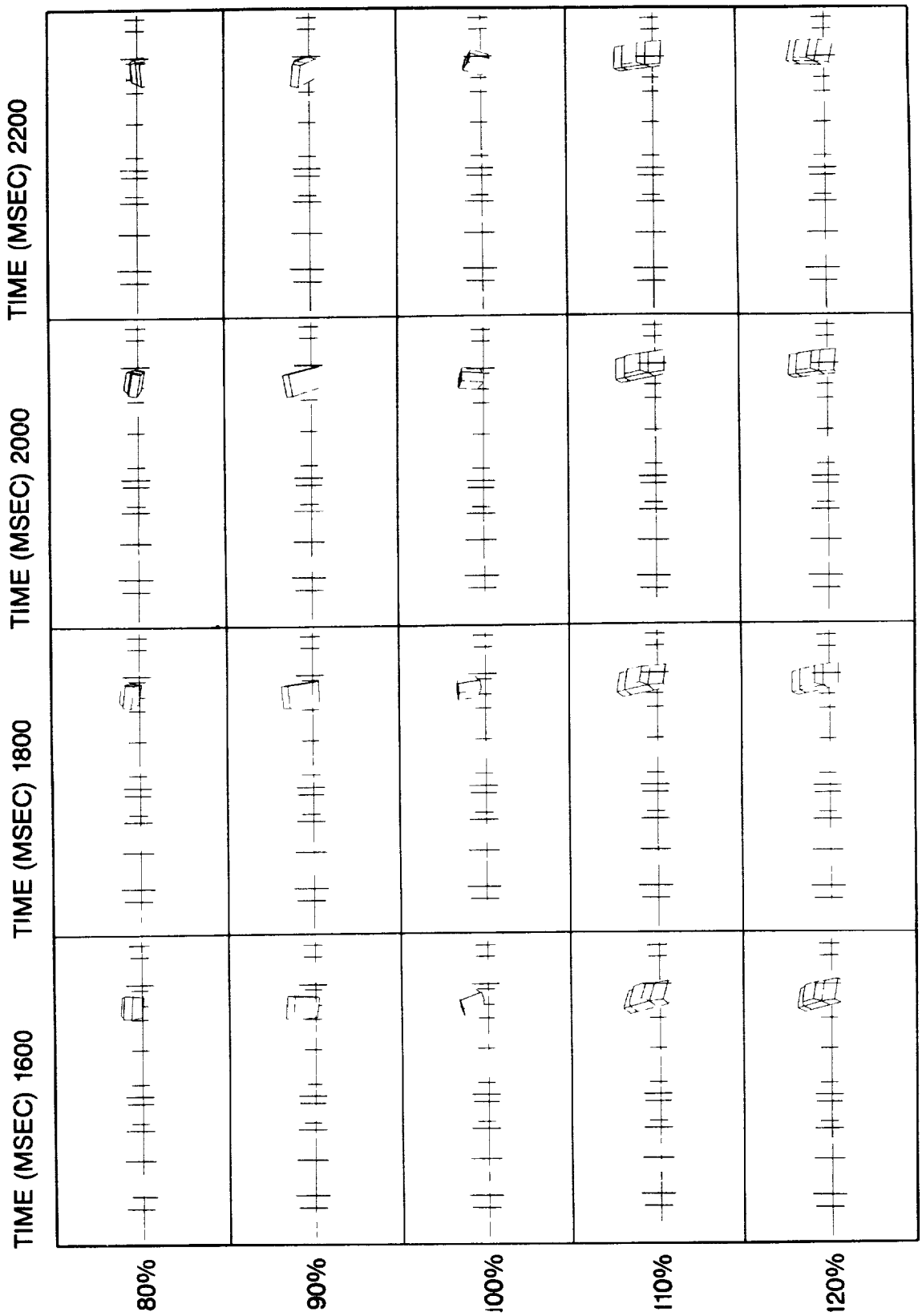

Figure 11 continued

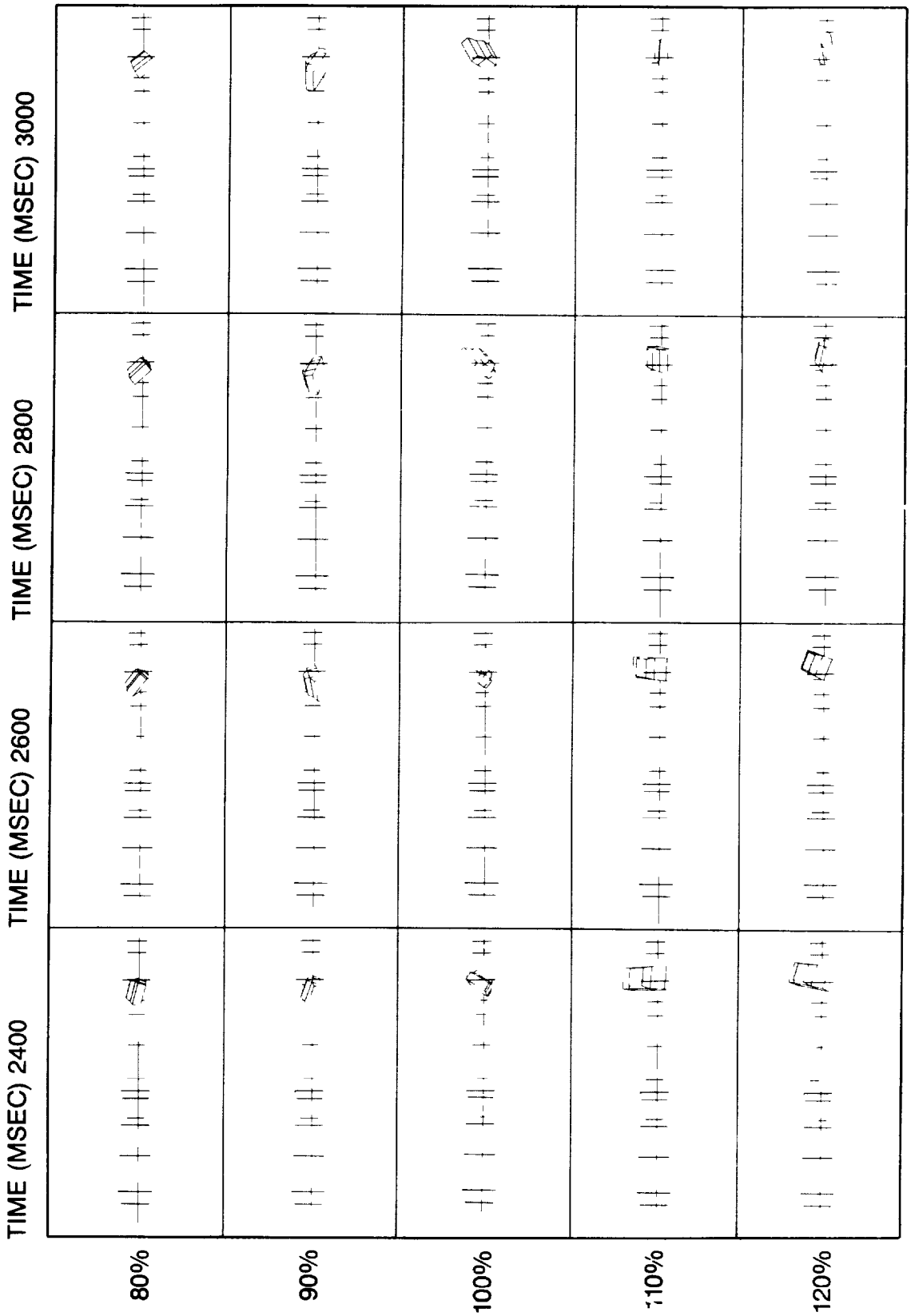

Figure 11 continued

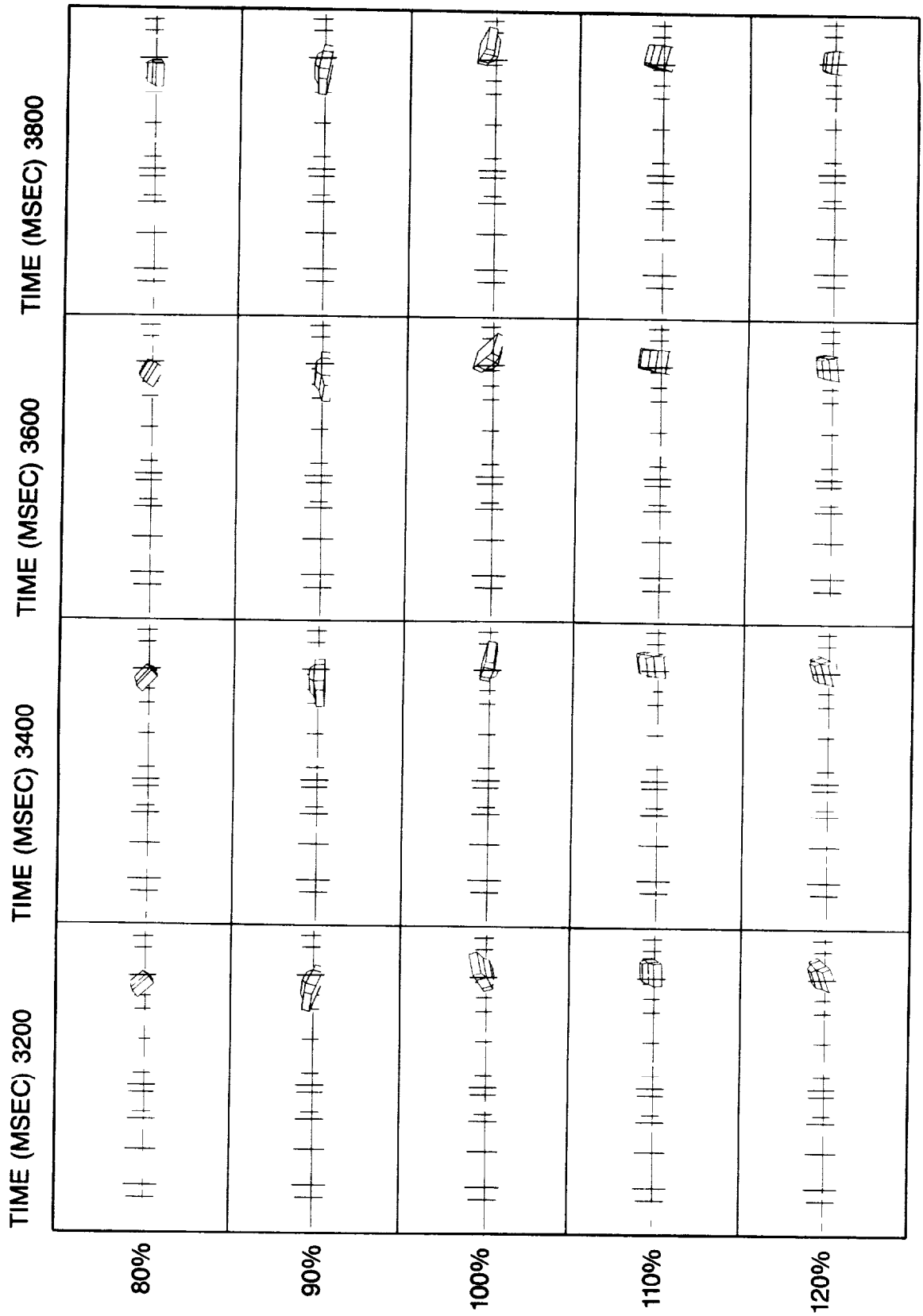

Figure 11 continued

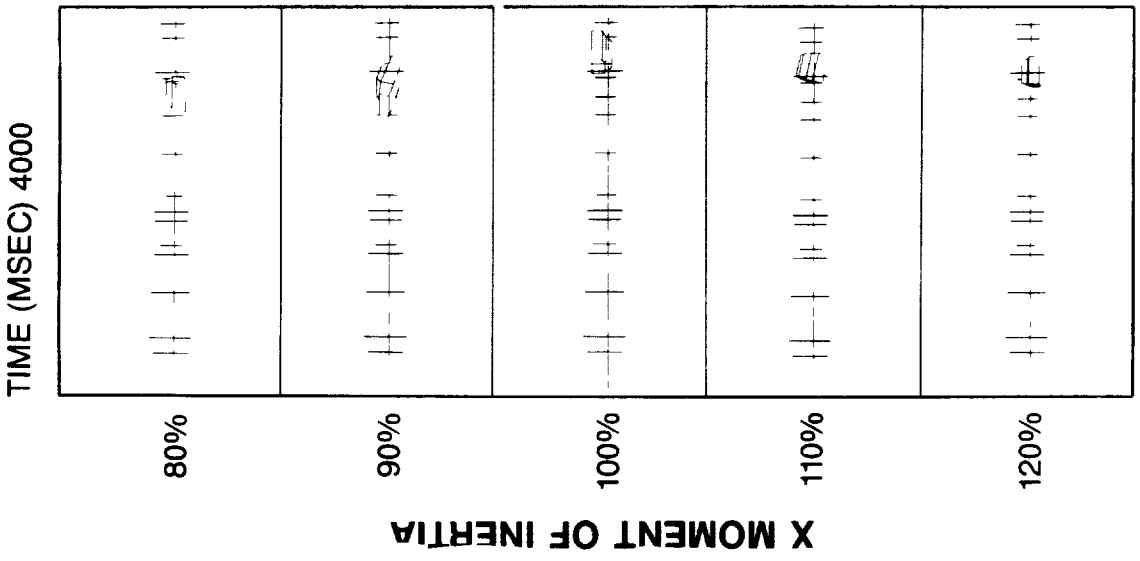

Figure 11 continued

moments, the roll rate is less. While the roll rate difference is small, it leads to a slightly different vehicle orientation when the vehicle is striking the ground at approximately 1000 msec. Due to the different orientation, the contact force with the ground is applied at different points on the vehicle leading to nose up pitching motion for reduced Ixx moments and nose down pitching motion for increased Ixx moments. For the baseline case, pitching motion is minimally affected. The increased pitching motion both for the lower and higher Ixx moment cases results in reduced rolling motion of the vehicle with the final position at 4000 msec for these cases being one half turn less than for the baseline case.

What these results seem to indicate is that changes in inertial properties minimally affect the motion of the vehicle directly. However, the slight modifications that result from inertial property differences can result in drastically different vehicle motion trajectories due to ground contact interactions with different parts of the vehicle. These effects are highly nonlinear in that slight positional differences can result in significantly different moment applications to the vehicle due to contact forces which in turn can substantially modify the vehicle's rotational trajectory.

Effects of Friction Coefficient Variation

In the baseline simulation, the friction coefficient used for the ground-vehicle contact (not including the tires) was 0.40. For this parametric study, three other simulations were run with the value of the friction coefficient being 0.30, 0.20, and 0.10. The VIEW plots of these simulations are shown in Figure 12. The results of this parametric study are more predictable than those of the first. With a lower friction coefficient, the vehicle would be expected to slide along the ground more and roll less. This is the case for the first 1600 msec. As the friction coefficient is progressively lowered, the vehicle has greater linear velocity and lower angular velocity. After 1600 msec, however, the vehicles in these simulations maintain contact with the ground while the baseline vehicle is off the ground surface. This results in the vehicles with the lower friction coefficients "catching up" to the baseline vehicle. It is clearly seen from these illustrations that the value of the coefficient of friction has a significant impact on the linear and particularly the angular velocity of the resulting motion.

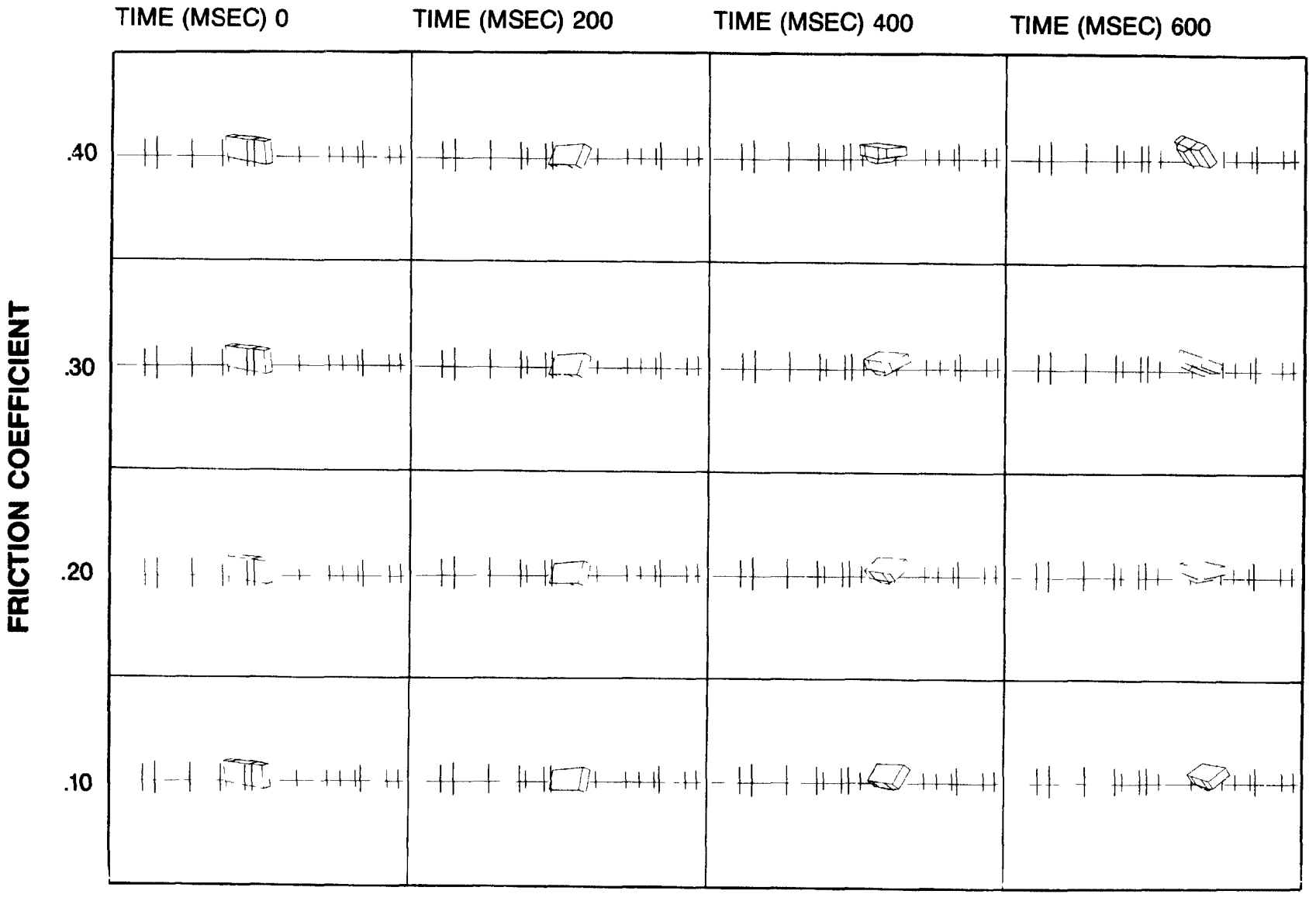

Figure 12 Friction Coefficient Parameter Study
Vehicle Motion

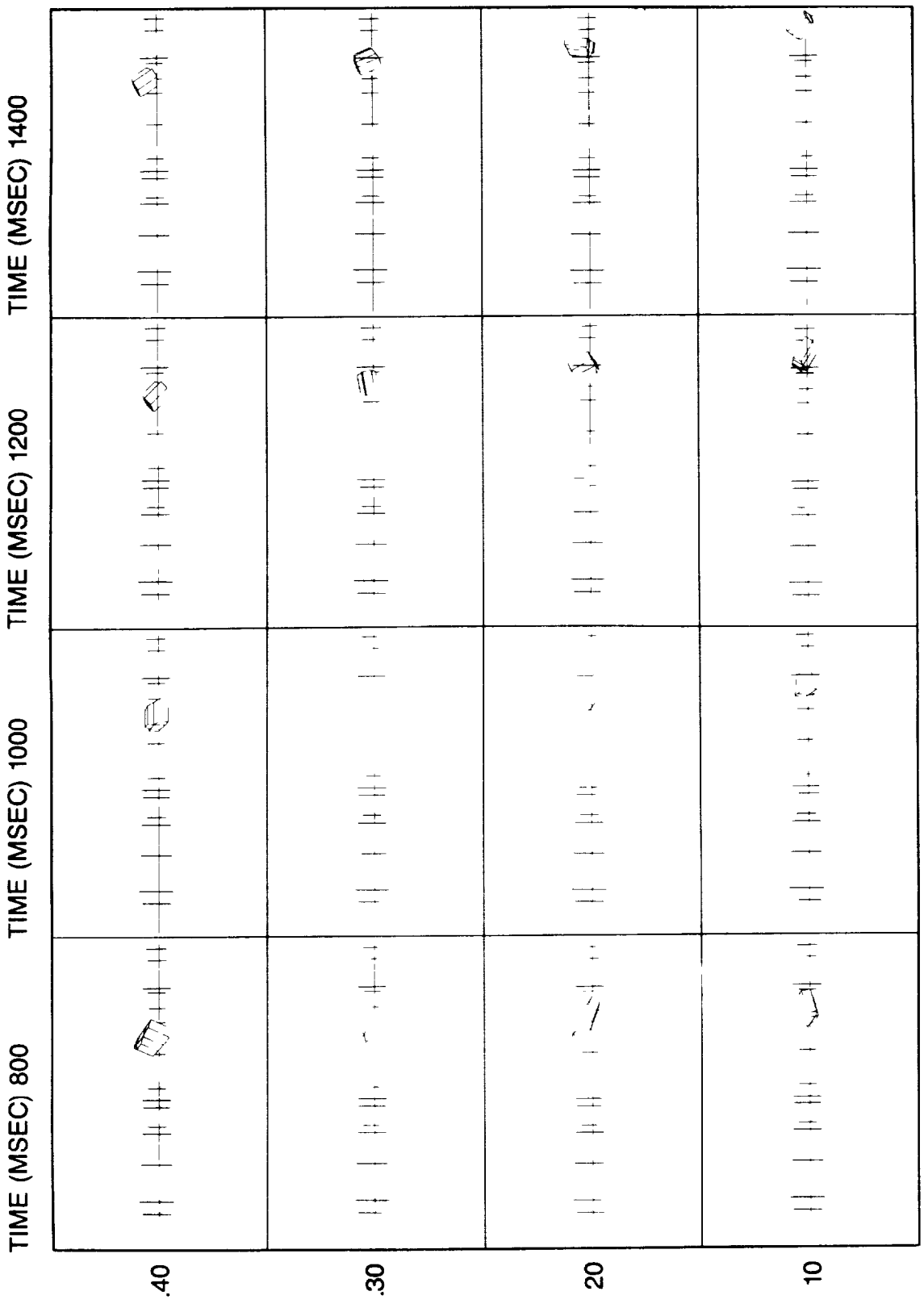

Figure 12 continued

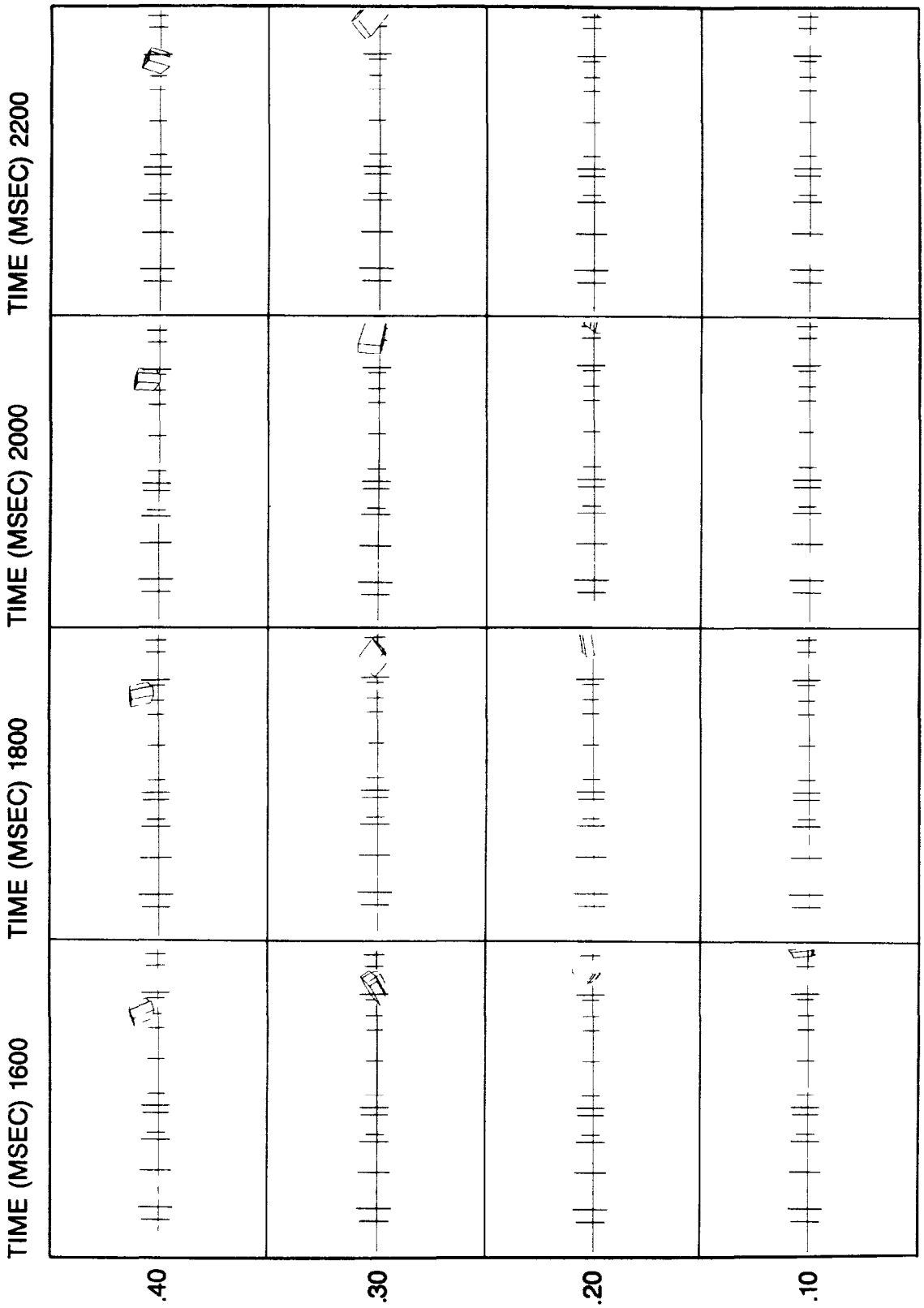

Figure 12 continued

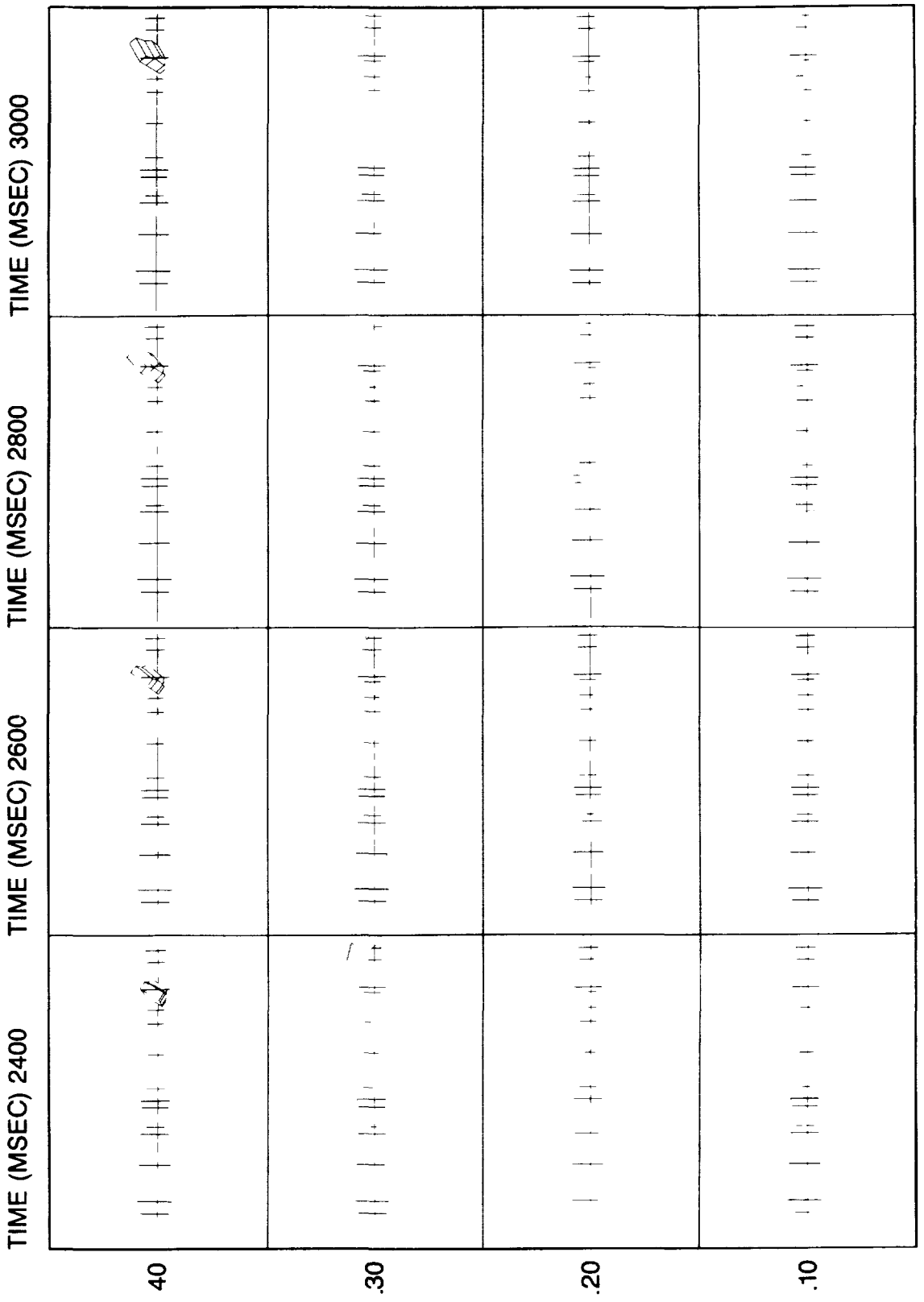

Figure 12 continued

GUARDRAIL IMPACT ROLLOVER

DESCRIPTION OF TEST

In order to further refine the techniques of vehicle simulation using the ATB model, the motion of a vehicle in a second, more complex rollover crash test was predictively simulated. Performed by the Southwest Research Institute (SWRI), this test used a 1982 Dodge Aries (essentially the same type of car as in the first test) for the test vehicle [Ref. 11]. Rollover was initiated by running the vehicle up the turned-down end of a guardrail at 60 mph. The longitudinal centerline of the vehicle was offset from the guardrail, and the resulting motion of the car was quite violent; four complete revolutions about the vehicle's longitudinal axis were made in approximately 4.5 seconds. The layout of the test is illustrated in Figure 13. As in the previous test, high-speed cameras placed around the test area recorded the motion for future study. The view from the camera placed above and behind the car was used for comparisons to the simulation.

MODIFICATIONS TO VEHICLE DESIGN

Although the type of vehicle used in this test was the same as in the previous test, certain modifications to the vehicle description were necessary due to the nature of the crash and also to improve the amount of energy absorption. One change

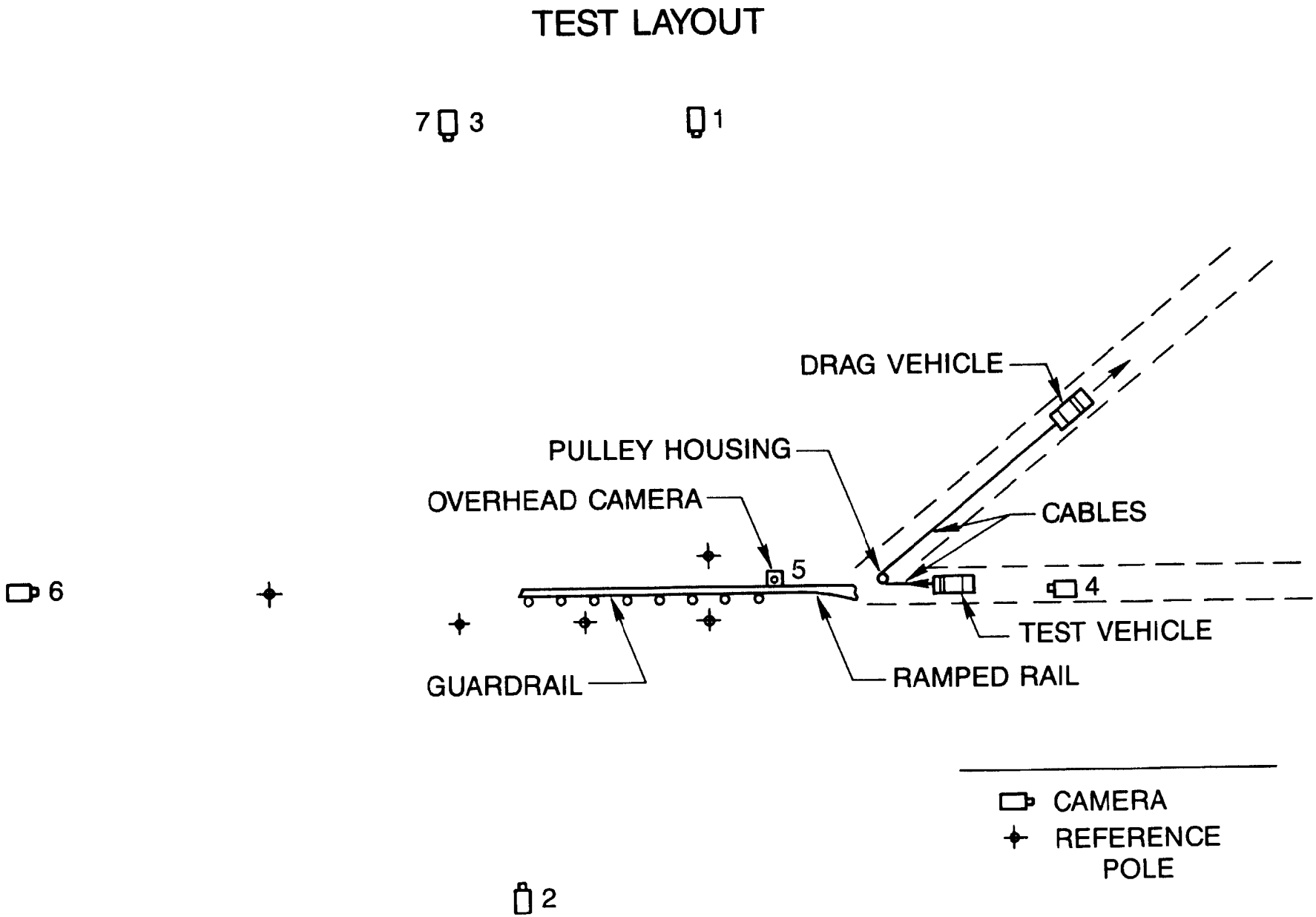

Figure 13 Layout of Guardrail Impact Rollover Test

involved attaching an additional hyper llipsoid to the vehicle segment to represent the bottom surfaces of the car (axles, drive train, etc.) (Figure 14). This was necessary in order to simulate the contact forces of the guardrail as the vehicle initially rode up the guardrail.

The other major modification made to the vehicle description was the method of defining the force-deflection characteristics. For the first test simulation, the force-deflection characteristics were defined in terms of a loading function, an energy absorption function, and a permanent deflection function. Because of the way that the program calculates the unloading curve from these functions, an insufficient amount of energy was being absorbed for these simulations as evidenced by the bouncing of the vehicle in the simulation. An alternate method of defining these characteristics is available with the ATB model using functions that are dependent upon both the deflection and the rate of deflection. With the rate-dependent functions option, a greater percentage of the available kinetic energy can be absorbed through surface contacts. The characteristics of the vehicle contacts with the ground and guardrail were defined with rate-dependent functions so that the vehicle would not bounce as high as in the first simulation and so it would stop its motion in the correct time period.

VEHICLE CONTACT (HYPER) ELLIPSOIDS

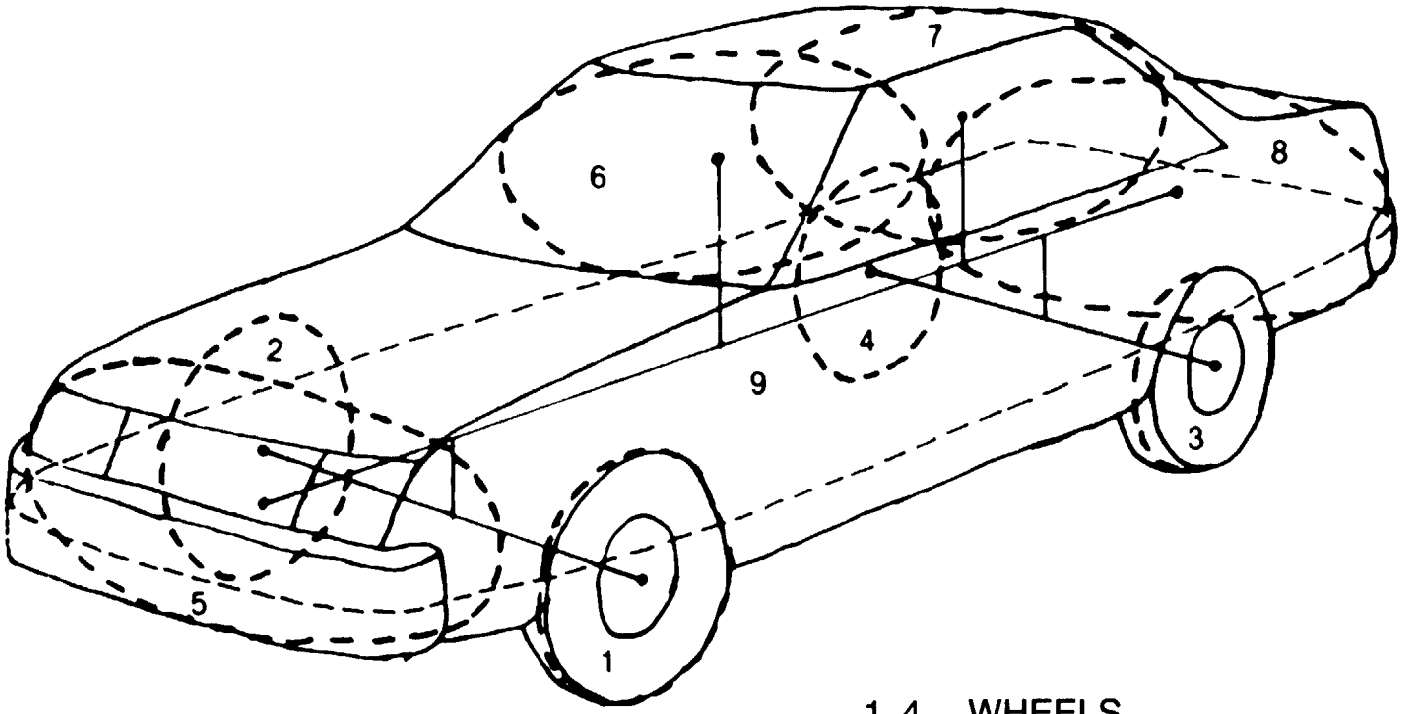

1–4	WHEELS
5	FRONT BUMPER
6	FRONT ROOF
7	REAR ROOF
8	REAR BUMPER
9	UNDERSIDE

Figure 14 Vehicle Contact (Hyper)Ellipsoids

DESCRIPTION OF GUARDRAIL

The guardrail surfaces were modeled with planes that were attached to the ground segment. The posts that held the guard rail were modeled with separate segments that were joined to the ground by locked joints and had surfaces defined by ellipsoids. Since in the actual test, the car appeared to hit only three of the posts, only these three were included in the simulation. The dimensions and locations of the guardrail and posts were determined by measurements taken at the test site. The force-deflection characteristics of the guardrail and posts were defined with rate-dependent functions which were estimated by observing the post deformation and vehicle motion in the film. As with the ground contacts, the functions were refined through an iterative process of preliminary simulations.

INITIAL CONDITIONS

Time zero was defined as a point just before the vehicle impacted the end of the guardrail. The position and orientation of the car at this instant were measured at the test site and verified from analysis of the film. The linear velocity of the vehicle at time zero had a value of 60 mph, and there was no angular rotation until the car hit the guardrail.

The complete input file from this simulation is included in the Appendix.

SIMULATION RESULTS

VIEW Graphics

The position of camera number 4 (see Figure 13), located behind and above the ramp end of the guardrail, was used in the VIEW program to obtain images of the simulation comparable to those of the actual test. Figure 15 contains the pictures of both the simulation and the film starting with time zero and continuing at 300 msec intervals. As the car proceeds up the end of the guardrail, the left side of the car is elevated off the ground, thus initiating the rolling motion. By comparing the time-sequence pictures of the actual and predicted vehicle motion, one can see that they are very similar. Both vehicles rolled four total revolutions, the final orientation and linear position appear to be the same, and the progression of positions during the crash was very similar. The greatest difference between the two vehicle motions is in the timing of the angular motion. Initially, the simulated vehicle has a slightly greater roll velocity than the actual vehicle, probably due to minor differences in the force-deflection characteristics of the guardrail-vehicle interaction. At approximately 1100 msec, the angular roll velocity of the actual vehicle abruptly increases and by 1700 msec the roll positions of the simulated and actual vehicles are aligned. The actual vehicle continues to roll faster until about 3500 msec, after which time about a 180 degree roll position difference is

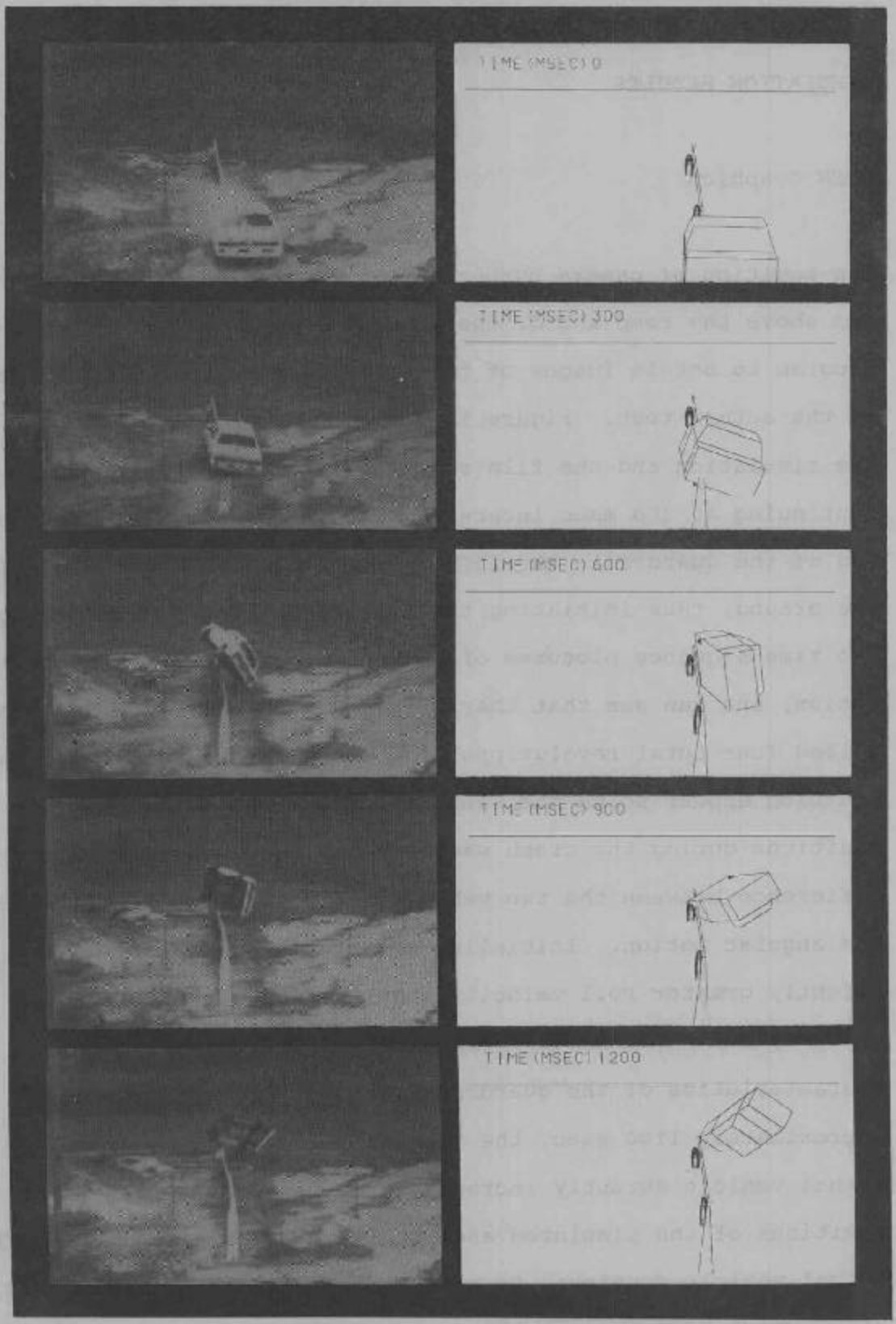

Figure 15 Guardrail Impact Rollover Test
Test Film and Simulated Motion

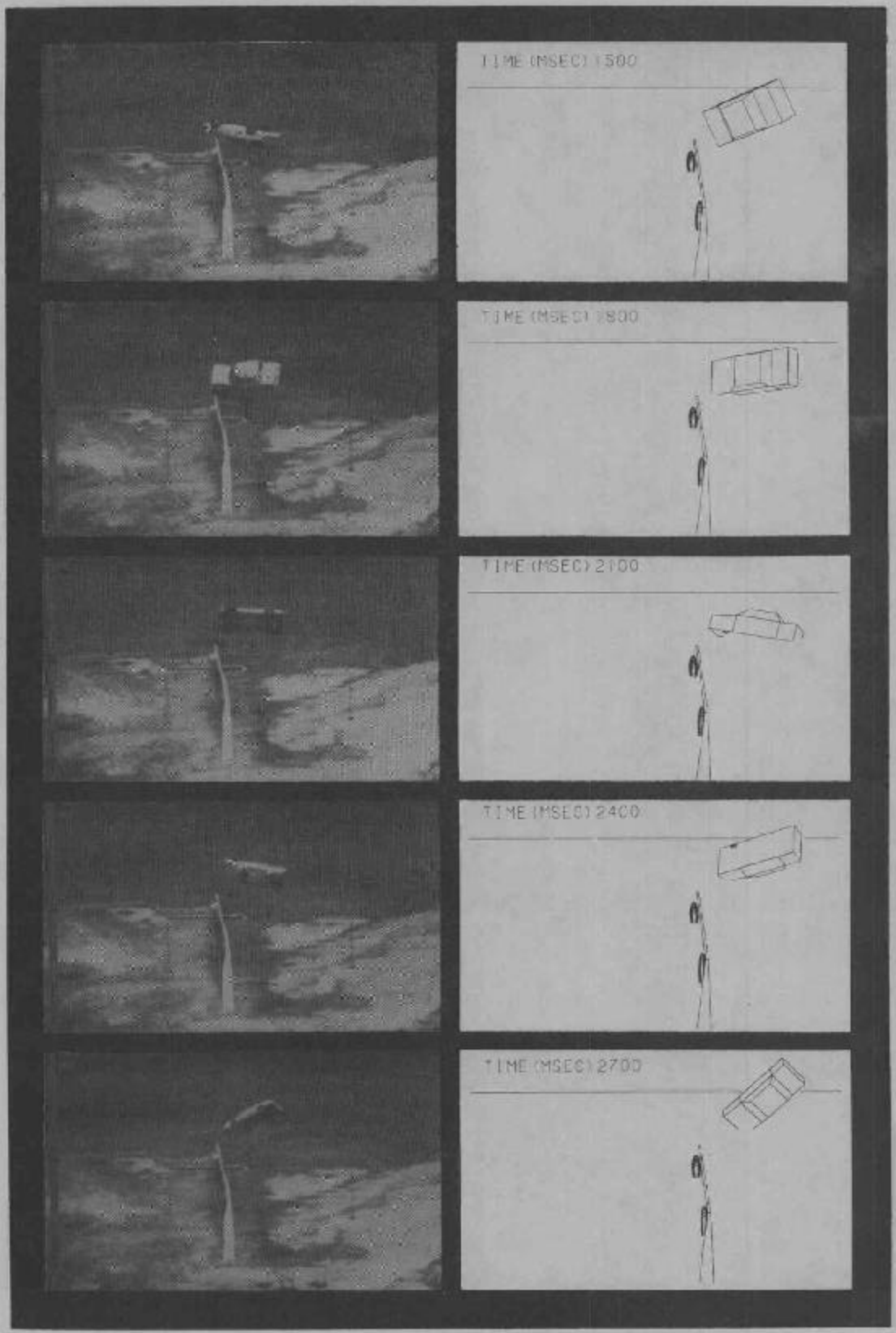

Figure 15 continued

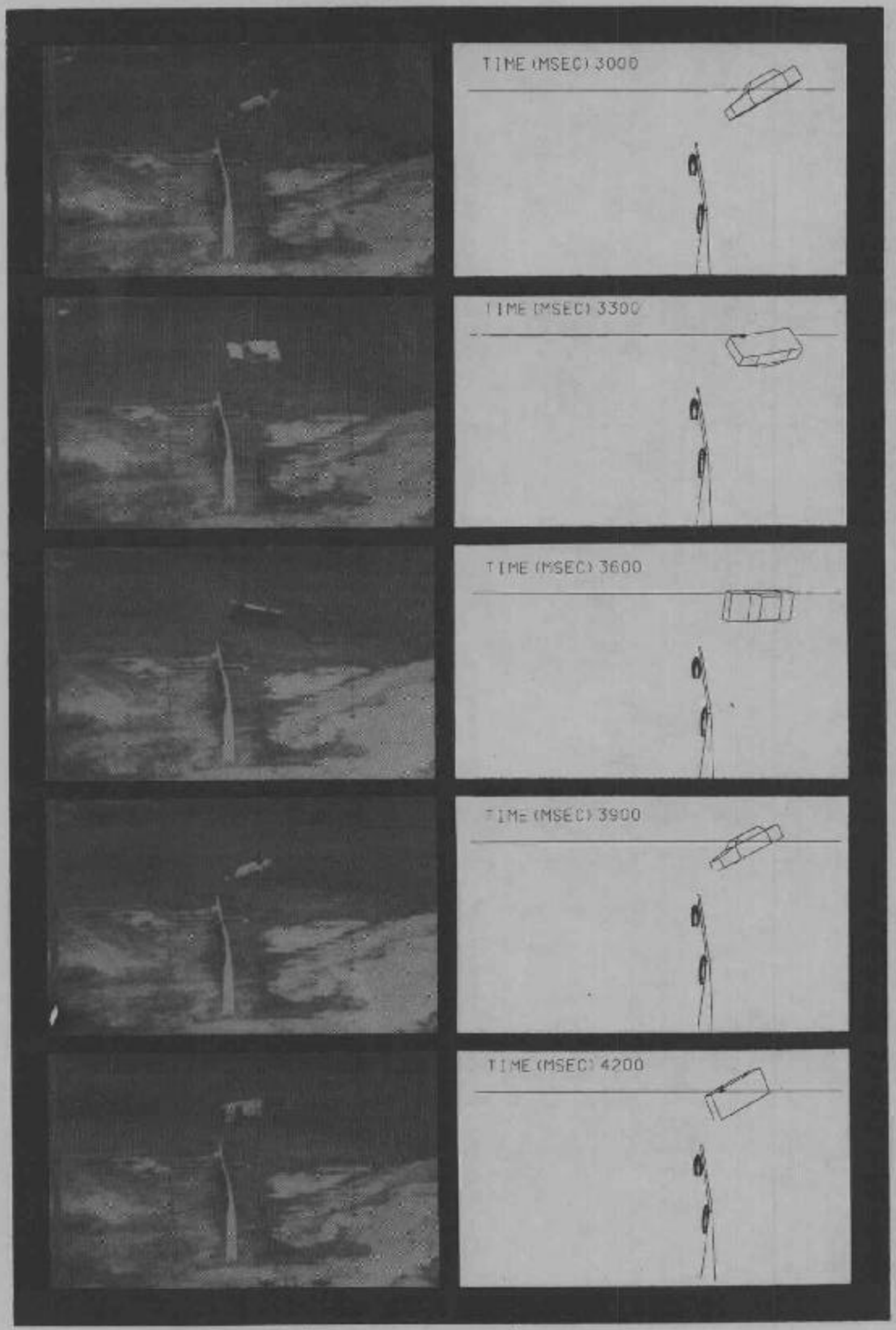

Figure 15 continued

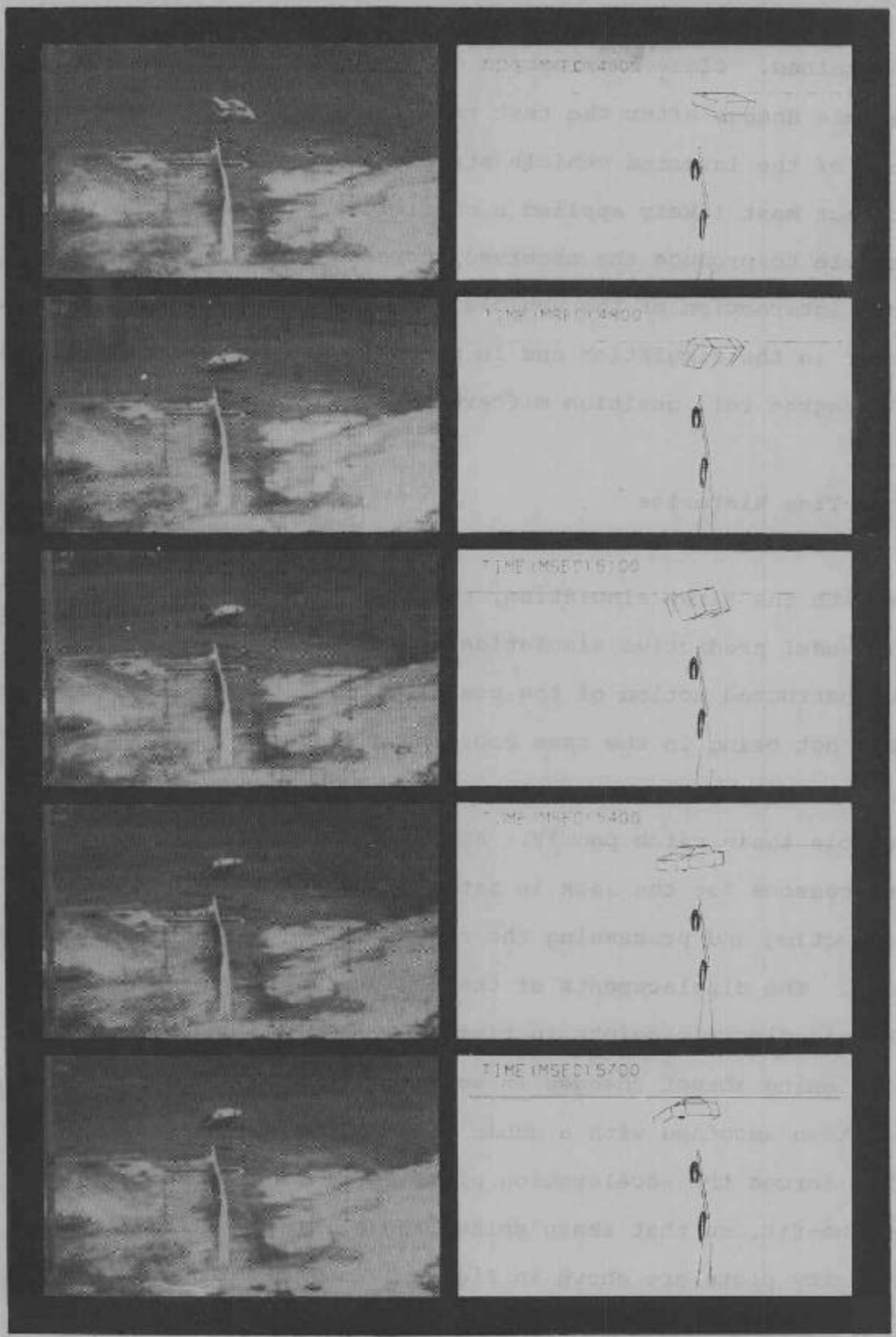

Figure 15 continued

maintained. Close examination of the photographic records and vehicle damage after the test revealed that at 1100 msec the hood of the inverted vehicle struck the guardrail. This contact most likely applied a sufficient roll moment to the vehicle to produce the observed increase in roll velocity. This interaction of the vehicle hood with the guardrail did not occur in the simulation and is probably the cause for the final 180 degree roll position difference.

Data Time Histories

As with the first simulation, the time history plots from the ATB model predictive simulation are compared to those from the reconstructed motion of the crash test due to the accelerometer data not being in the same coordinate system. As shown in Figure 16, the linear acceleration curves of the CG of the vehicle again match poorly. As explained previously, one of the reasons for the lack in matching is the method used for collecting and processing the reconstructed motion displacement data. The displacements of the vehicle were recorded only at certain discrete points in time, leaving open the possibility of missing abrupt changes in motion. This displacement data was then smoothed with a cubic spline-fitting routine [Ref. 3]. This forces the acceleration plots to be continuous, linear spline-fit, so that sharp spikes are eliminated. The linear velocity plots are shown in Figure 17. These plots match quite well in spite of the length and complexity of the simulation

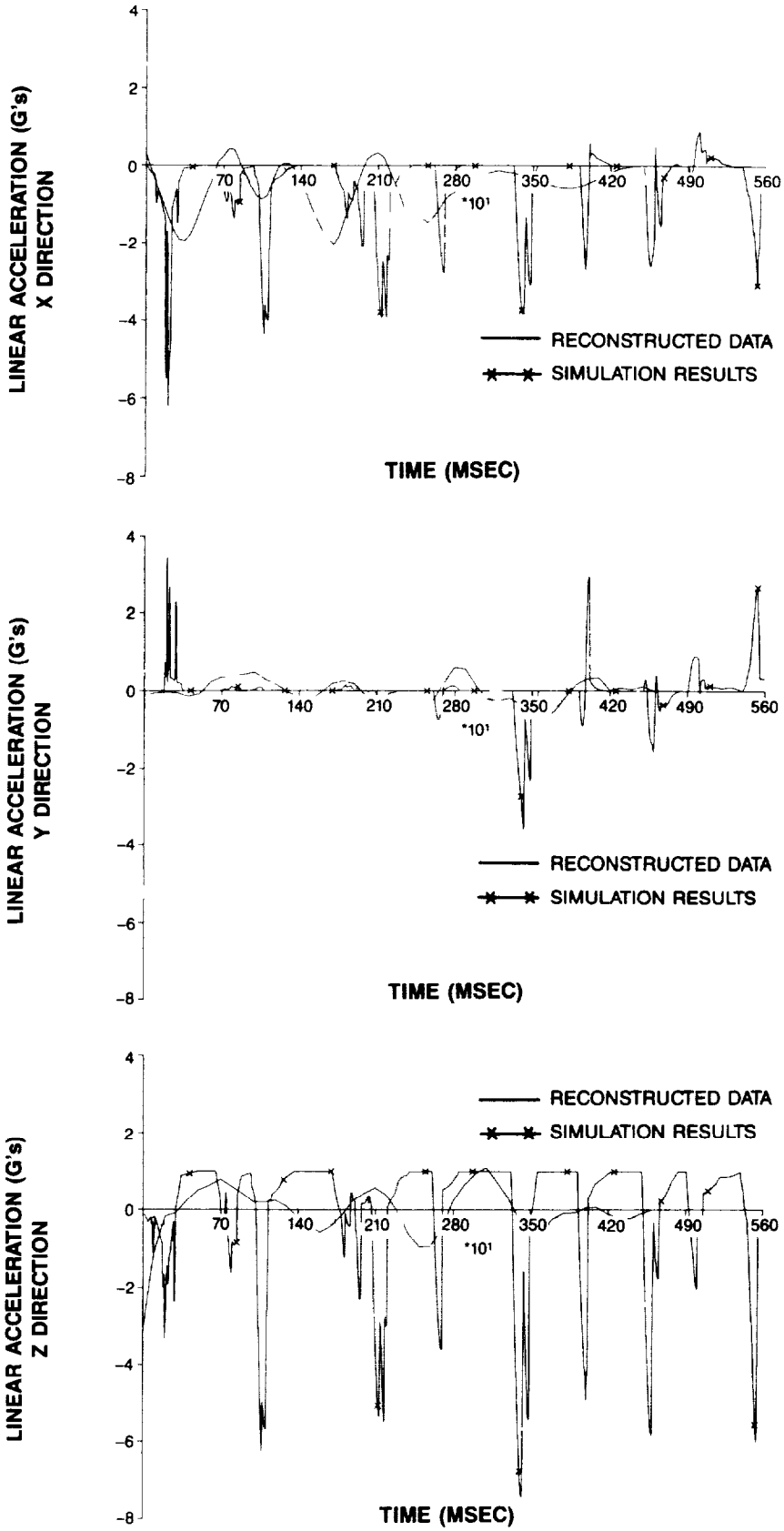

Figure 16 Reconstructed and Simulated Linear Accelerations

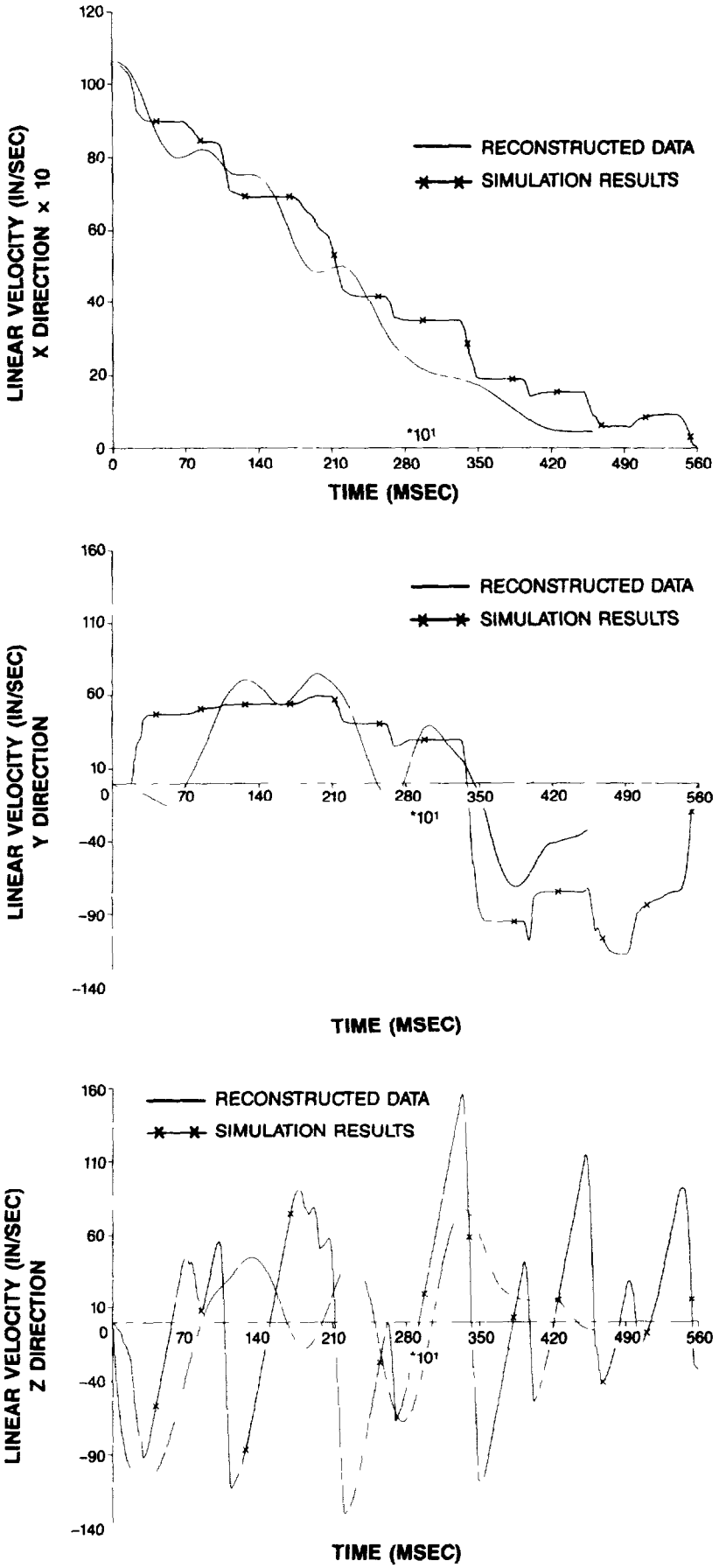

Figure 17 Reconstructed and Simulated Linear Velocities

and of the number of estimations and approximations made. Both the X and Y components of linear velocity go to zero at the end of the simulation. Since the vehicle is still rocking, the Z component of linear velocity has a non-zero value at the end of the simulation. The "stairstep" shape of the X component of velocity curve is due to the vehicle impacting the ground or guardrail (a sudden drop in velocity) and then bouncing in the air (a flat plateau). Figure 18 includes the three components of linear displacement. These also match very well, with the simulation displacements being slightly larger in the X and Y directions. All three of the plots show the smoothing effect in the reconstructed data.

The angular acceleration plots (Fig. 19) match relatively poorly, as is expected. Again, the reconstructed data is much smoother than the simulation data. The angular velocity data agrees much better (Fig. 20). From the X axis angular velocity plot, one can see the phase shift of the rolling motion as described in the previous section. From approximately 1200 to 4100 msec, the simulation motion is roughly 400 msec behind the reconstructed motion. Figure 21 shows very good agreement in the angular displacement plots. The roll plot again reflects the phase shift and also shows that both the reconstructed and the simulated vehicle rolled four complete revolutions.

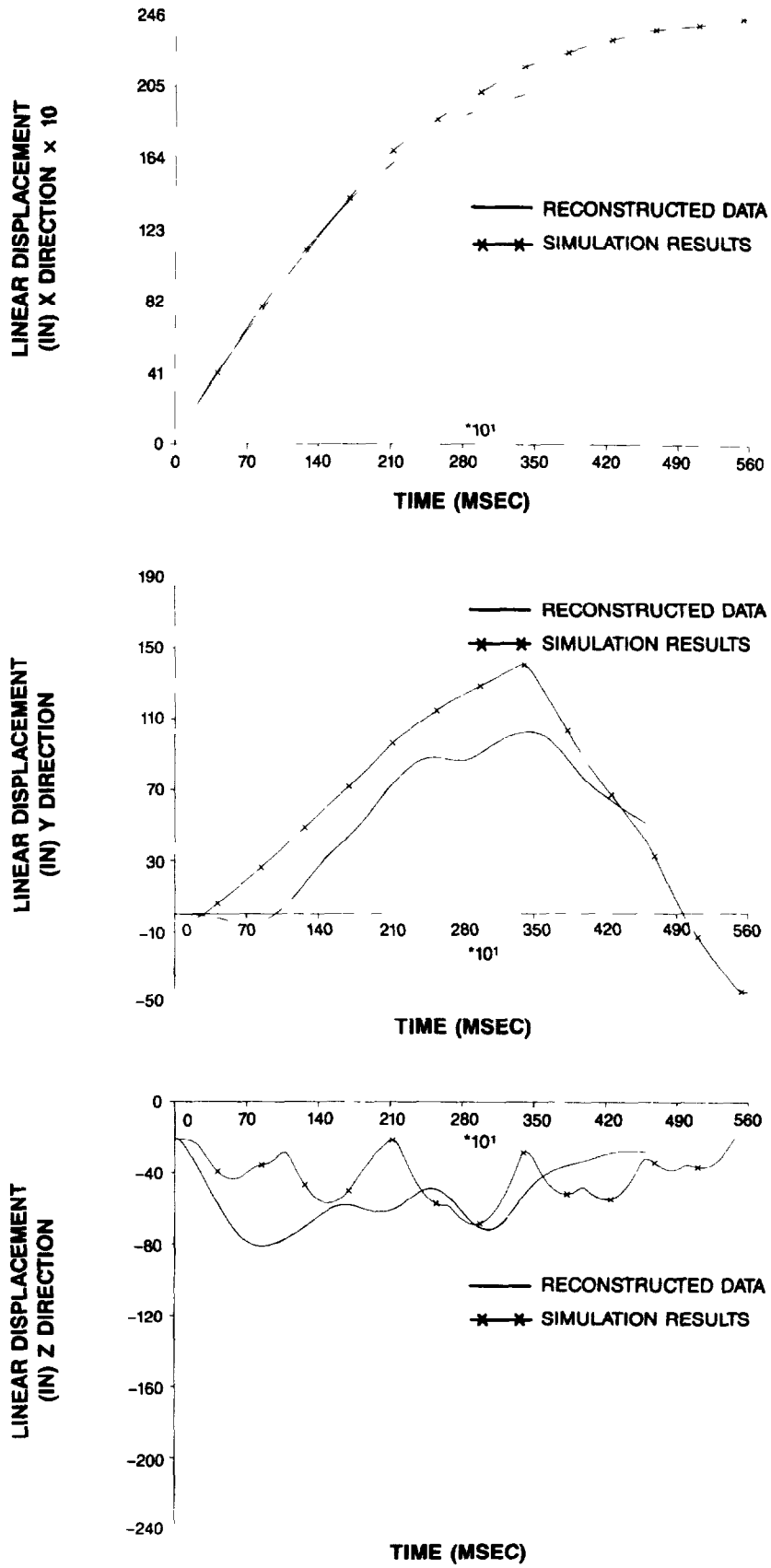

Figure 18 Reconstructed and Simulated Linear Displacements

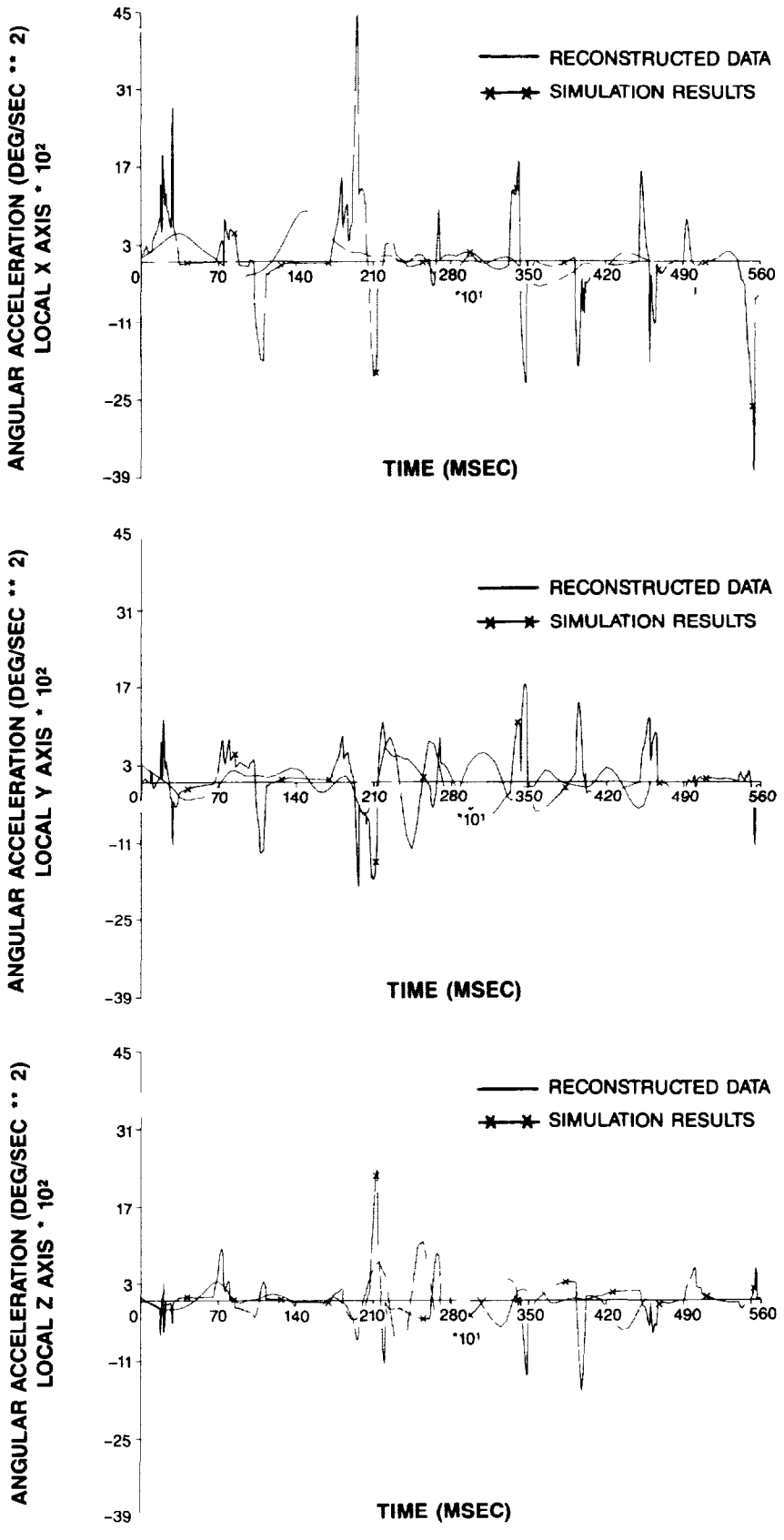

Figure 19 Reconstructed and Simulated Angular Accelerations

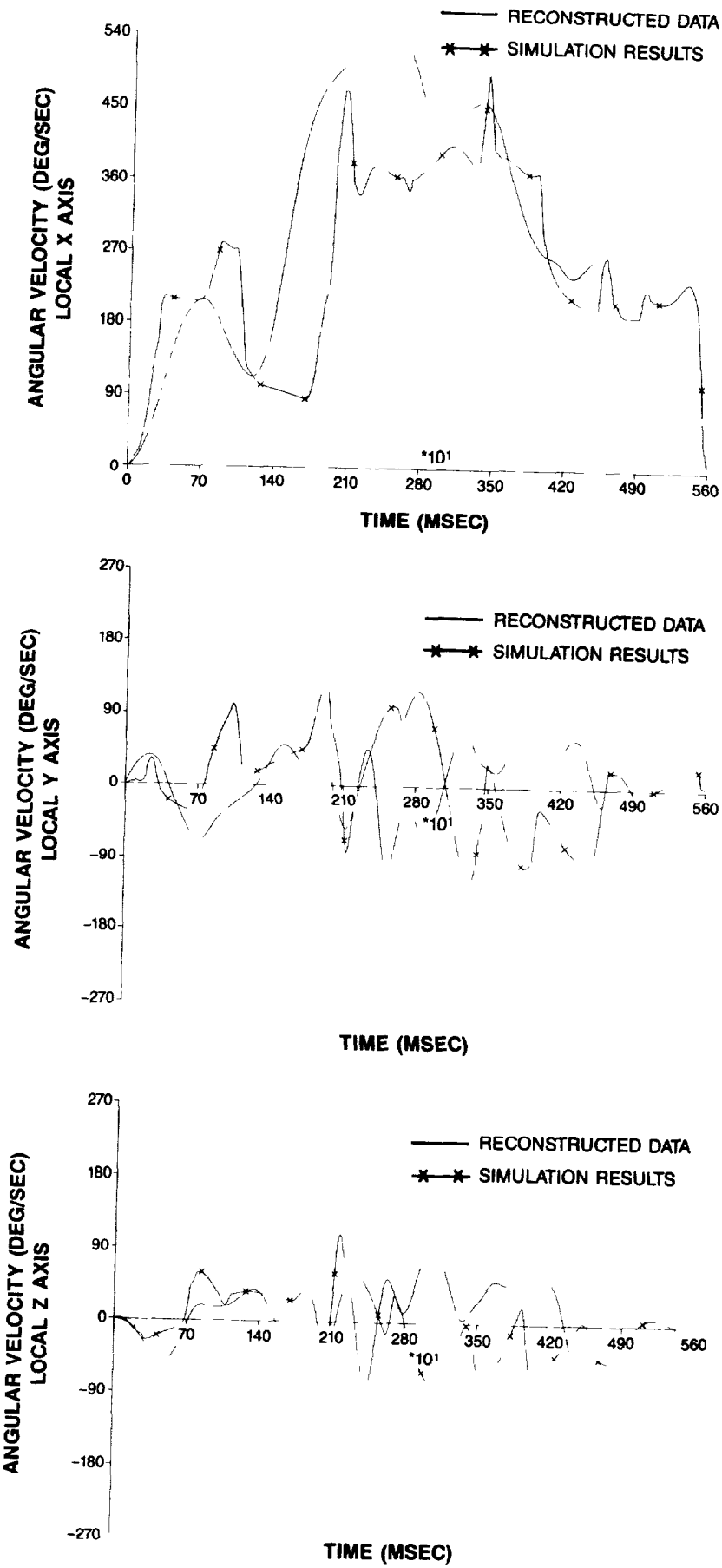

Figure 20 Reconstructed and Simulated Angular Velocities

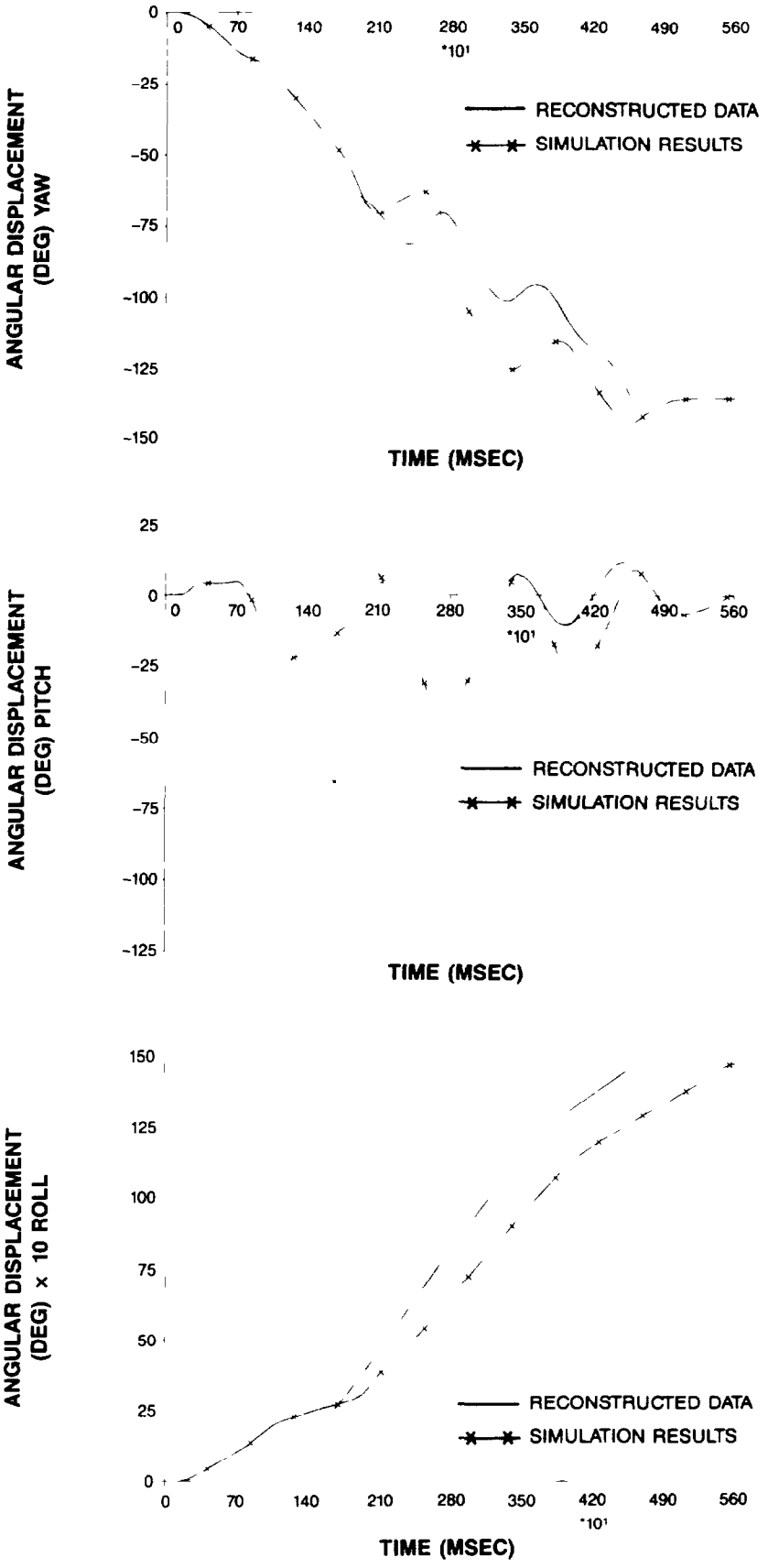

Figure 21 Reconstructed and Simulated Angular Displacements

The kinetic energy plots are shown in Figure 22. These clearly show the improvement in kinetic energy absorption over the first vehicle rollover simulation by using the rate-dependent functions option of the ATB model. As with the first test, the amount of kinetic energy associated with linear motion is more than an order of magnitude greater than that associated with angular motion. Indicated on the kinetic energy plots are the major surface contacts occurring throughout the simulation. This shows that large drops in linear kinetic energy occur when the vehicle impacts external objects or surfaces. The effect of vehicle impacts on the angular kinetic energy depends a great deal upon where the contact occurs on the vehicle body, therefore it is difficult to determine any relationship between the timing of impacts and the angular motion of the vehicle. Both the linear and angular kinetic energy for the simulation go to zero at 5600 msec, indicating that the vehicle has come to rest.

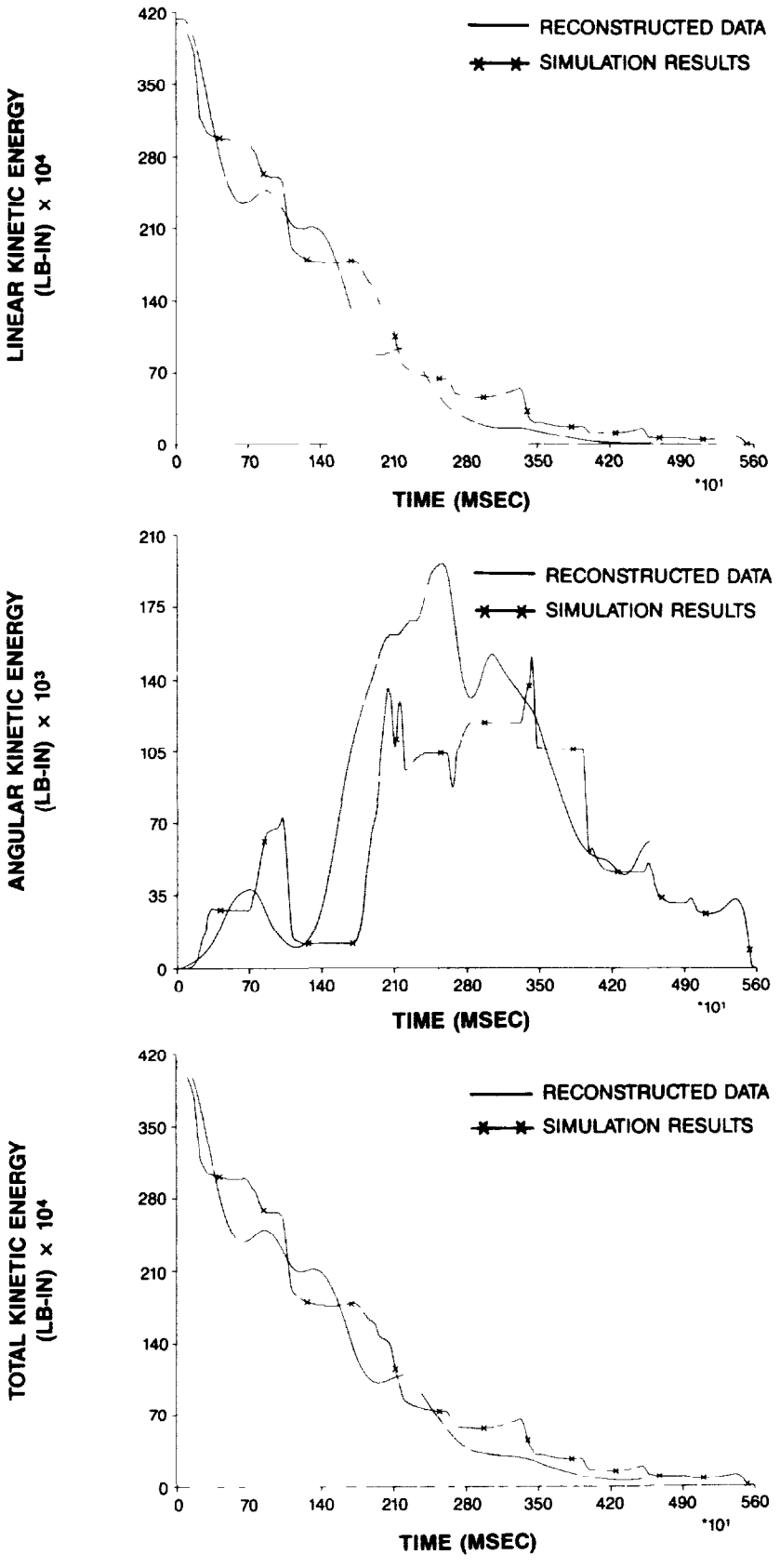

Figure 22 Reconstructed and Simulated Kinetic Energies

CONCLUSIONS

The Articulated Total Body model was originally developed to simulate human and dummy dynamics during short-term (100 - 400 msec) crash situations. However, there are no inherent characteristics of the program or the manner of prescribing the input data which limit one to these types of simulations. The main objectives of this project were to 1) determine the feasibility of using the ATB model to predictively simulate the motion of an automobile during relatively complex, long-term events (2.0 - 6.0 seconds), 2) develop the methodology to perform these simulations, and 3) validate the process using the results of actual crash tests.

The simulations of two vehicle rollover tests were successfully performed. The second, more complex crash test, a guardrail impact rollover, was simulated more accurately due to two major factors: 1) the first simulation brought forth many of the potential difficulties that can be encountered during this type of simulation and, 2) the rate-dependent functions option of the ATB, not used for the first simulation, allowed the surface contacts to more closely duplicate the actual energy-absorption process. The success of these simulations demonstrates the feasibility of using the ATB program to predict the motion of a vehicle during a complex event such as a rollover.

Many factors are important for the successful performance of a vehicle simulation. One of them is a good prescription of the vehicle's exterior surfaces, since the calculations of the contact forces and points of application of these forces depend upon the shapes of the contacting surfaces. Although an exact duplication is probably not practical, a careful combination of hyperellipsoids and ellipsoids should give an approximation adequate for these simulations.

Other critical factors are the inertial properties of the vehicle and the prescriptions of the force-deflection characteristics for the various surface interactions. This point is illustrated by the parameter studies performed on the first crash test. The motion of the vehicle was dramatically altered with a 10 percent change in the value of the principal moment of inertia about the X axis. The differences in the motions became greater as the simulations progressed, as would be expected. Perhaps the most surprising result of this parameter study was that when the roll moment of inertia was altered, the pitching motion of the vehicle greatly changed. This study illustrates the importance of accurate measurements of all inertial data. It is recommended that future research of this type use measured inertial data instead of approximations.

The guardrail impact rollover simulation matched quite well with the actual vehicle motion, especially considering the approximations of the vehicle surface, the inertial properties,

and the force-deflection characteristics. This was shown in both the visual graphics comparisons and also in the kinematic data comparisons. The results of these two vehicle rollover simulations clearly demonstrate the feasibility of using the ATB model as a predictive simulator for gross vehicle motion for a crash/rollover event. Further refinements of the methodology and better defined vehicle and vehicle/ground contact properties would further improve the capability. Specific areas of future work that would most benefit this methodology are: 1) Modeling of wheel suspension systems; 2) developing a library of contact properties between a vehicle and various ground surfaces, and vehicle geometric and inertial properties; and 3) generating a set of baseline simulations that can be used for parameter variation studies or as a starting point for simulations of different situations. All of these refinements require the collection of appropriate experimental data, including suspension system properties for extremely high and unconventional force applications, crush characteristics of vehicle roofs and other surface parts, and overall vehicle motion data during various crash/rollover events. With the resulting improved and validated physical property data and modeling methodology, the ATB model would have many applications as a predictive vehicle dynamics simulation tool, including parameter studies of vehicle and crash characteristics. Reconstruction of actual motor vehicle rollover accidents will require an extensive series of simulations of real-world crashes before the computer model would be suitable.

MAY 9, 1988 IRSIN= 0 IRSOUT= 0 RSTIME = 0.0000 CARDS A

SOUTHWEST RESEARCH INSTITUTE GUARDRAIL INDUCED ROLLOVER TEST SIMULATION
1982 DODGE ARIES - V(0) = 60 MPH - 0 DEG YAW, PITCH, AND ROLL

UNITL = IN UNITM = LB. UNITT = SEC GRAVITY VECTOR = (0.0000, 0.0000, 386.0880) G = 386.0880

NDINT = 6 NSTEPS = 2900 DT =0.002000 H0 =0 000250 HMAX =0 000500 HMIN =0.000008

NPRT ARRAY

1	2	3	4	5	6	7	8	9	10	11	12	13	14	15	16	17	18	19	20	21	22	23	24	25	26	27	28	29	30	31	32	33	34	35	36
5	0	50	0	0	0	0	0	0	0	0	0	0	0	0	1	0	0	0	0	0	0	0	0	0	-3	0	0	0	0	0	0	0	0	0	1

CRASH VICTIM 1982 DODGE ARIES 4 SEGMENTS 0 JOINTS PAGE 2

CARD B.1
CARDS B.2

SEGMENT I	SYM	PLOT	WEIGHT (LB.)	PRINCIPAL MOMENTS OF INERTIA (LB-SEC.**2-IN.) X	Y	Z	SEGMENT CONTACT ELLIPSOID SEMIAXES (IN.) X	Y	Z	CENTER (IN.) X	Y	Z	PRINCIPAL AXES (DEG) YAW	PITCH	ROLL
1	CAR	C	2826.000	3897.0000**********			1.000	1.000	1.000	1 000	1 000	1.000	0.00	0.00	0.00
2	PST1	P	1.000	1 0000	1.0000	1.0000	3.500	3 500	17 000	0 000	0.000	0.000	0 00	0.00	0.00
3	PST9	0	1.000	1.0000	1.0000	1.0000	2 000	6 000	15.000	0 000	0 000	0 000	0.00	0.00	0.00
4	PS10	S	1.000	1 0000	1.0000	1.0000	2.000	6 000	15.000	0 000	0 000	0.000	0.00	0.00	0.00

SEGMENT INTEGRATION CONVERGENCE TEST INPUT CARDS B.6

SEGMENT NO. SYM	ANGULAR VELOCITIES (RAD/SEC.) MAG. TEST	ABS. ERROR	REL. ERROR	LINEAR VELOCITIES (IN./SEC.) MAG. TEST	ABS. ERROR	REL ERROR	ANGULAR ACCELERATIONS (RAD/SEC.**2) MAG. TEST	ABS. ERROR	REL ERROR	LINEAR ACCELERATIONS (IN./SEC.**2) MAG. TEST	ABS. ERROR	REL. ERROR
1 CAR	0.010	0.010	0.0010	0.010	0.010	0.0010	0.010	0.010	0.0010	0.010	0.010	0.0010
2 PST1	0.000	0.000	0.0000	0.000	0.000	0.0000	0.000	0.000	0.0000	0.000	0.000	0.0000
3 PST9	0.000	0.000	0.0000	0.000	0.000	0.0000	0.000	0.000	0.0000	0.000	0.000	0.0000
4 PS10	0.000	0.000	0.0000	0.000	0.000	0.0000	0.000	0.000	0.0000	0.000	0.000	0.0000

VEHICLE DECELERATION INPUTS PAGE 4

POST NUMBER 1

YAW	PITCH	ROLL	VIPS	VTIME	XD(X)	XD(Y)	XD(Z)	NATAB	ATO	ADT	MSEG
0.000	0.000	0.000	0.000	0.000	261.000	-23.000	-14.000	-3	0.000000	1.000000	2

SPLINE FIT TABULAR INPUT

LTYPE = 1 LFIT = 2 NPTS = 3

TIME(SEC.)	LINEAR POSITION (IN.) X	Y	Z	ANGULAR POSITION (DEG) YAW	PITCH	ROLL
0.00000	261.000	-23.000	-14.000	0.000	0.000	0.000
1.00000	261.000	-23.000	-14.000	0.000	0.000	0.000
2.00000	261.000	-23.000	-14.000	0.000	0.000	0.000

VEHICLE LINEAR TIME HISTORY POST NUMBER 1

TIME (MSEC)	LINEAR DECELERATIONS (G'S) X	Y	Z	LINEAR VELOCITIES (IN./SEC.) X	Y	Z	LINEAR DISPLACEMENTS (IN.) X	Y	Z
0 000	0.000	0.000	0.000	0.000	0.000	0.000	261 000	-23.000	-14.000
1000.000	0.000	0.000	0.000	0.000	0.000	0.000	261.000	-23.000	-14.000
2000.000	0 000	0.000	0.000	0.000	0.000	0.000	261.000	-23.000	-14.000

VEHICLE ANGULAR TIME HISTORY POST NUMBER 1

TIME (MSEC)	ANGULAR ACCELERATIONS (DEG/SEC.**2) X	Y	Z	ANGULAR VELOCITIES (DEG/SEC.) X	Y	Z	ANGULAR DISPLACEMENTS (DEG) YAW	PITCH	ROLL
0.000	0.000	0.000	0.000	0.000	0.000	0.000	0 000	0.000	0.000
1000.000	0.000	0.000	0.000	0.000	0.000	0.000	0.000	0.000	0.000
2000.000	0.000	0 000	0.000	0.000	0 000	0.000	0.000	0.000	0.000

VEHICLE DECELERATION INPUTS
POST NUMBER 9

YAW	PITCH	ROLL	VIPS	VTIME	XD(X)	XD(Y)	XD(Z)	NATAB	ATO	ADT	MSEG
0.000	0 000	0.000	0 000	0 000	861 000	-25 500	-10.500	-3	0.000000	1.000000	3

SPLINE FIT TABULAR INPUT

LTYPE = 1 LFIT = 2 NPTS = 3

TIME(SEC.)	LINEAR POSITION (IN.) X	Y	Z	ANGULAR POSITION (DEG) YAW	PITCH	ROLL
0.00000	861.000	-25.500	-10.500	0.000	0.000	0.000
1.00000	861.000	-25.500	-10.500	0.000	0.000	0.000
2.00000	861.000	-25.500	-10.500	0.000	0.000	0.000

1

VEHICLE LINEAR TIME HISTORY POST NUMBER 9

TIME (MSEC)	LINEAR DECELERATIONS (G'S) X	Y	Z	LINEAR VELOCITIES (IN./SEC.) X	Y	Z	LINEAR DISPLACEMENTS (IN.) X	Y	Z
0.000	0.000	0.000	0.000	0.000	0.000	0.000	861.000	-25.500	-10.500
1000.000	0.000	0.000	0.000	0.000	0.000	0.000	861.000	-25.500	-10.500
2000.000	0.000	0.000	0.000	0.000	0.000	0.000	861.000	-25.500	-10.500

VEHICLE ANGULAR TIME HISTORY POST NUMBER 9

TIME (MSEC)	ANGULAR ACCELERATIONS (DEG/SEC.**2) X	Y	Z	ANGULAR VELOCITIES (DEG/SEC.) X	Y	Z	ANGULAR DISPLACEMENTS (DEG) YAW	PITCH	ROLL
0.000	0.000	0.000	0.000	0 000	0.000	0 000	0.000	0.000	0.000
1000.000	0.000	0.000	0.000	0.000	0.000	0 000	0.000	0.000	0.000
2000.000	0.000	0.000	0.000	0.000	0.000	0.000	0.000	0.000	0.000

VEHICLE DECELERATION INPUTS PAGE 10
POST NUMBER 10

YAW	PITCH	ROLL	VIPS	VTIME	XD(X)	XD(Y)	XD(Z)	NATAB	ATO	ADT	MSEG
0 000	0.000	0.000	0 000	0 000	936.000	-25 500	-10 500	-3	0.000000	1 000000	4

SPLINE FIT TABULAR INPUT

LTYPE = 1 LFIT = 2 NPTS = 3

	LINEAR POSITION (IN)			ANGULAR POSITION (DEG)		
TIME(SEC.)	X	Y	Z	YAW	PITCH	ROLL
0 00000	936.000	-25.500	-10.500	0.000	0.000	0.000
1.00000	936.000	-25.500	-10.500	0.000	0.000	0.000
2.00000	936.000	-25.500	-10 500	0 000	0 000	0.000

PAGE 11
VEHICLE LINEAR TIME HISTORY POST NUMBER 10 PAGE NO. 1

TIME	LINEAR DECELERATIONS (G'S)			LINEAR VELOCITIES (IN./SEC.)			LINEAR DISPLACEMENTS (IN.)		
(MSEC)	X	Y	Z	X	Y	Z	X	Y	Z
0.000	0.000	0.000	0.000	0.000	0.000	0.000	936.000	-25.500	-10.500
1000.000	0.000	0.000	0.000	0.000	0.000	0 000	936.000	-25.500	-10.500
2000.000	0.000	0.000	0.000	0.000	0.000	0.000	936 000	-25.500	-10.500

VEHICLE ANGULAR TIME HISTORY POST NUMBER 10 PAGE 12
PAGE NO 1

TIME	ANGULAR ACCELERATIONS (DEG/SEC.**2)			ANGULAR VELOCITIES (DEG/SEC.)			ANGULAR DISPLACEMENTS (DEG)		
(MSEC)	X	Y	Z	X	Y	Z	YAW	PITCH	ROLL
0.000	0.000	0.000	0.000	0.000	0.000	0.000	0.000	0.000	0.000
1000.000	0.000	0.000	0.000	0 000	0.000	0 000	0.000	0.000	0 000
2000.000	0.000	0.000	0.000	0.000	0.000	0.000	0.000	0.000	0.000

VEHICLE DECELERATION INPUTS
DUMMY VEHICLE

YAW	PITCH	ROLL	VIPS	VTIME	XD(0)	XD(Y)	XD(Z)	NATAB	ATO	ADT	MSEG
0.000	0.000	0.000	0.000	0.000	0.000	0.000	-20.000	-3	0.000000	1.000000	0

SPLINE FIT TABULAR INPUT

LTYPE = 2 LFIT = 1 NPTS = 3

TIME(SEC.)= 0.0000 X= INITIAL LINEAR POSITION (IN.) 0.000 Y= 0.000 Z= 0.000

X= INITIAL ANGULAR POSITION (DEG) 0.000 Y= 0.000 Z= 0.000

TIME(SEC.)	LINEAR VELOCITY (IN./SEC.) X	Y	Z
0.00000	0.000	0 000	0 000
1.00000	0.000	0.000	0 000
2.00000	0 000	0.000	0.000

ANGULAR VELOCITY (DEG/SEC.) X	Y	Z
0 000	0.000	0.000
0.000	0.000	0.000
0 000	0.000	0 000

VEHICLE LINEAR TIME HISTORY DUMMY VEHICLE

TIME (MSEC)	LINEAR DECELERATIONS (G'S) X	Y	Z	LINEAR VELOCITIES (IN./SEC.) X	Y	Z	LINEAR DISPLACEMENTS (IN.) X	Y	Z
0.000	0.000	0.000	0.000	0.000	0.000	0 000	0.000	0.000	0.000
1000.000	0.000	0.000	0.000	0.000	0.000	0 000	0.000	0.000	0.000
2000.000	0.000	0 000	0.000	0 000	0 000	0.000	0.000	0.000	0.000

VEHICLE ANGULAR TIME HISTORY DUMMY VEHICLE

TIME (MSEC)	ANGULAR ACCELERATIONS (DEG/SEC **2) X	Y	Z	ANGULAR VELOCITIES (DEG/SEC) X	Y	Z	ANGULAR DISPLACEMENTS (DEG) YAW	PITCH	ROLL
0 000	0 000	0.000	0.000	0 000	0 000	0 000	0.000	0.000	0 000
1000 000	0.000	0.000	0.000	0 000	0.000	0.000	0.000	0.000	0.000
2000.000	0.000	0.000	0 000	0 000	0.000	0.000	0 000	0 000	0 000

CARDS D.2

NPL	NBLT	NBAG	NELP	NQ	NSD	NHRNSS	NWINDF	NJNTF	NFORCE
11	0	0	9	0	0	0	0	0	0

PLANE INPUTS

PLANE NO. 1 GROUND PLANE (FRONT)

	X	Y	Z
POINT 1	-3000.0000	-3000.0000	0.0000
POINT 2	-3000.0000	3000.0000	0.0000
POINT 3	140.0000	-3000.0000	0.0000

PLANE NO. 2 GROUND PLANE (REAR)

	X	Y	Z
POINT 1	140.0000	-3000.0000	0.0000
POINT 2	140.0000	3000.0000	0.0000
POINT 3	5000.0000	-3000.0000	0.0000

PLANE NO 3 RAIL TOP 1 (STRAIGHT

	X	Y	Z
POINT 1	261.0000	-16.5000	-24.0000
POINT 2	1161.0000	-16.5000	-24.0000
POINT 3	261.0000	-19.5000	-24.0000

PLANE NO. 4 RAIL TOP 2 (STRAIGHT

	X	Y	Z
POINT 1	261.0000	-16.5000	-24.0000
POINT 2	1161.0000	-16.5000	-24.0000
POINT 3	261.0000	-19.5000	-24.0000

PLANE NO 5 RAIL +SIDE 1 (STRAIG			
	X	Y	Z
POINT 1	261.0000	-16.5000	-24 0000
POINT 2	261 0000	-16.5000	-12.0000
POINT 3	1161 0000	-16.5000	-24.0000

PLANE NO 6 RAIL +SIDE 2 (STRAIG			
	X	Y	Z
POINT 1	261.0000	-16.5000	-24 0000
POINT 2	261.0000	-16.5000	-12.0000
POINT 3	1161.0000	-16.5000	-24 0000

PLANE NO. 7 RAIL TOP 1 (SLANTED)			
	X	Y	Z
POINT 1	-12.0000	-18.5000	0.0000
POINT 2	261.0000	-16.5000	-24.0000
POINT 3	-12.0000	-28.2500	0.0000

PLANE NO. 8 RAIL TOP 2 (SLANTED)			
	X	Y	Z
POINT 1	-12.0000	-18.5000	0 0000
POINT 2	261.0000	-16.5000	-24.0000
POINT 3	-12.0000	-28.2500	0.0000

PLANE NO 9 RAIL +SIDE 1 (SLANTE			
	X	Y	Z
POINT 1	-12.0000	-18.5000	0.0000
POINT 2	-12 0000	-18.5000	12.0000
POINT 3	261.0000	-16.5000	-24.0000

CARDS D.2

PLANE NO 10 RAIL +SIDE 2 (SLANTE

	X	Y	Z
POINT 1	-12.0000	-18.5000	0.0000
POINT 2	-12.0000	-18.5000	12.0000
POINT 3	261.0000	-16.5000	-24.0000

PLANE NO 11 GROUND PLANE (REAR)

	X	Y	Z
POINT 1	140.0000	-3000.0000	0.0000
POINT 2	140.0000	3000.0000	0.0000
POINT 3	5000.0000	-3000.0000	0.0000

ADDITIONAL ELLIPSOID INPUT

CARDS D.5

NO	SEMIAXES (IN.) X	Y	Z	OFFSET (IN.) X	Y	Z	ROTATION (DEG) YAW	PITCH	ROLL	POWER		
1	12.000	4.000	12.000	37 400	-28.800	12 300	0.000	0.000	0.000	0.	0.	0
7	12.000	4.000	12.000	37 400	28 800	12.300	0.000	0.000	0.000	0	0	0
8	12.000	4.000	12.000	-62.200	-28.500	12.300	0.000	0.000	0.000	0	0.	0.
9	12.000	4.000	12.000	-62 200	28 500	12.300	0.000	0.000	0 000	0	0.	0.
10	18.000	34.000	8 000	55.400	0 000	0.800	0.000	0.000	0.000	10	10.	10.
11	25.500	28.800	8.800	-1.400	0 000	-24 300	0.000	-19.000	0.000	0	0	0
12	19.000	28.500	10.000	-51 400	0.000	-23.800	0.000	28.000	0 000	0.	0.	0.
13	20.000	34.000	10 000	-82.200	0.000	-2.500	0.000	0 000	0.000	10	10.	10.
14	68.800	34.300	14.700	-13.400	0.000	-1.200	0.000	0.000	0 000	8.	8	8.

BODY SEGMENT SYMMETRY INPUT

CARD D.7

SEG NO.	1	2	3	4
NSYM(J)	0	0	0	0

FUNCTION NO 6 REAR SUSPENSION STIF NTI(6) = 1 CARDS E

D0	D1	D2	D3	D4
0 0000	100.0000	0 0000	0 0000	1 0000

FIRST PART OF FUNCTION - 5TH DEGREE POLYNOMIAL

A0	A1	A2	A3	A4	A5
0.000000	132.625000	0.000000	0 000000	0.000000	0 000000

FUNCTION NO 7 SLANTED GUARDRAIL ST NTI(7) = 12 CARDS E

D0	D1	D2	D3	D4
0.0000	20.0000	0.0000	0 0000	0.0000

FIRST PART OF FUNCTION - 5TH DEGREE POLYNOMIAL

A0	A1	A2	A3	A4	A5
0 000000	0.000000	42 200000	0 000000	0.000000	0 000000

FUNCTION NO. 8 FRONT SUSPENSION STI NTI(8) = 23

CARDS E

D0	D1	D2	D3	D4
0.0000	100.0000	0.0000	0.0000	1 0000

FIRST PART OF FUNCTION - 5TH DEGREE POLYNOMIAL

A0	A1	A2	A3	A4	A5
0.000000	220.625000	0.000000	0.000000	0.000000	0 000000

FUNCTION NO. 9 BODY STIFFNESS NTI(9) = 34

CARDS E

D0	D1	D2	D3	D4
0.0000	30.0000	0.0000	0.0000	1.0000

FIRST PART OF FUNCTION - 5TH DEGREE POLYNOMIAL

A0	A1	A2	A3	A4	A5
0.000000	1250.000000	0 000000	0.000000	0.000000	0.000000

FUNCTION NO 10 GUARDRAIL STIFFNESS NTI(10) = 45 CARDS E

D0	D1	D2	D3	D4
0 0000	-25.0000	0.0000	0 0000	1 0000

FIRST PART OF FUNCTION - 8 TABULAR POINTS

D	F(D)
0.000000	0.0000
1.000000	1200.0000
2.000000	2400.0000
4.000000	3500.0000
6.000000	4000.0000
10.000000	4500.0000
18.000000	5000.0000
25.000000	5000.0000

FUNCTION NO. 11 POST STIFFNESS NTI(11) = 67 CARDS E

D0	D1	D2	D3	D4
0 0000	-25.0000	0.0000	0.0000	1 0000

FIRST PART OF FUNCTION - 8 TABULAR POINTS

D	F(D)
0.000000	0.0000
1 000000	2400.0000
2.000000	4800.0000
4.000000	7000.0000
6.000000	8000.0000
10.000000	9000.0000
18.000000	10000.0000
25.000000	10000.0000

FUNCTION NO 12 MULTIPLIER NTI(12) = 89 CARDS E

D0	D1	D2	D3	D4
-1000 0000	0.0000	20000.0000	0 0000	0 0000

FUNCTION IS CONSTANT20000 000000

FUNCTION NO 20 GUARDRAIL ABSORPTION NTI(20) = 94

CARDS E

D0	D1	D2	D3	D4
-1000.0000	-1000.0000	0.0000	0 0000	1 0000

FIRST PART OF FUNCTION - 4 TABULAR POINTS

D	F(D)
-1000.000000	0.5000
-1.000000	0.5000
0.000000	1 0000
1000.000000	1 0000

FUNCTION NO 21 BODY ABSORPTION NTI(21) = 108

D0	D1	D2	D3	D4
-1000.0000	-1000.0000	0.0000	0.0000	1.0000

FIRST PART OF FUNCTION - 4 TABULAR POINTS

D	F(D)
-1000 000000	0.1000
-1 000000	0 1000
0 000000	1 0000
1000 000000	1.0000

FUNCTION NO. 22 FRICTION = 0.40 NTI(22) = 122

CARDS E

D0	D1	D2	D3	D4
0.0000	0.0000	0.4000	0.0000	0.0000

FUNCTION IS CONSTANT 0.400000

FUNCTION NO. 23 FRICTION = 0.30 NTI(23) = 127

CARDS E

D0	D1	D2	D3	D4
0.0000	0.0000	0.3000	0 0000	0.0000

FUNCTION IS CONSTANT 0.300000

FUNCTION NO. 24 FRICTION = 0.80 (TIR NTI(24) = 132

CARDS E

D0	D1	D2	D3	D4
0.0000	0.0000	0.8000	0.0000	0.0000

FUNCTION IS CONSTANT 0.800000

FUNCTION NO 25 FRICTION = 0 0 (ROLL NTI(25) = 137 CARDS E

D0	D1	D2	D3	D4
0 0000	0.0000	0 0000	0 0000	0 0000

FUNCTION IS CONSTANT 0.000000

FUNCTION NO 26 R FACTOR = 0.80 T NTI(26) = 142 CARDS E

D0	D1	D2	D3	D4
0.0000	0.0000	0.8000	0 0000	0 0000

FUNCTION IS CONSTANT 0.800000

FUNCTION NO 27 R FACTOR = 0.90 NTI(27) = 147 CARDS E

D0	D1	D2	D3	D4
0 0000	0.0000	0.9000	0 0000	0 0000

FUNCTION IS CONSTANT 0.900000

FUNCTION NO 28 R FACTOR = 0.34 NTI(28) = 152

CARDS E

D0	D1	D2	D3	D4
0.0000	0.0000	0 3400	0.0000	0 0000

FUNCTION IS CONSTANT 0.340000

FUNCTION NO. 29 CONSTANT = 0.0 (SO NTI(29) = 157

CARDS E

D0	D1	D2	D3	D4
0.0000	0.0000	0.0000	0.0000	0.0000

FUNCTION IS CONSTANT 0.000000

FUNCTION NO. 30 R FACTOR = 0 60 NTI(30) = 162

CARDS E

D0	D1	D2	D3	D4
0.0000	0.0000	0.6000	0.0000	0.0000

FUNCTION IS CONSTANT 0.600000

FUNCTION NO 31 G FACTOR = 0 5 (BOD NTI(31) = 167 CARDS E

D0	D1	D2	D3	D4
0.0000	0.0000	0 5000	0 0000	0 0000

FUNCTION IS CONSTANT 0.500000

FUNCTION NO 32 G FACTOR = 0 20 NTI(32) = 172 CARDS E

D0	D1	D2	D3	D4
0 0000	0 0000	0 2000	0 0000	0 0000

FUNCTION IS CONSTANT 0.200000

FUNCTION NO 33 CONSTANT = 0 0 (HARD NTI(33) = 177 CARDS E

D0	D1	D2	D3	D4
0 0000	0 0000	0 0000	0 0000	1 0000

FUNCTION IS CONSTANT 0 000000

FUNCTION NO. 34 TIRE/GRND ABSORPTIO NTI(34) = 182

CARDS E

D0	D1	D2	D3	D4
-1000.0000	-1000.0000	0.0000	0.0000	1.0000

FIRST PART OF FUNCTION - 4 TABULAR POINTS

D	F(D)
-1000.000000	0.4700
-1.000000	0.4700
0.000000	1.0000
1000.000000	1.0000

FUNCTION NO. 35 FRICTION = 0.70 NTI(35) = 196

D0	D1	D2	D3	D4
0.0000	0.0000	0.7000	0.0000	0.0000

FUNCTION IS CONSTANT 0.700000

FUNCTION NO 36 FRICTION = 0 60 NTI(36) = 201 CARDS E

D0	D1	D2	D3	D4
0.0000	0 0000	0 6000	0 0000	0.0000

FUNCTION IS CONSTANT 0.600000

FUNCTION NO 40 BODY VISCOSITY NTI(40) = 206 CARDS E

D0	D1	D2	D3	D4
-2000.0000	-500 0000	0 0000	0 0000	1.0000

FIRST PART OF FUNCTION - 5 TABULAR POINTS

D	F(D)
-2000.000000	0.0000
-200 000000	0 0000
0 000000	0.0000
50 000000	200 0000
500 000000	1000 0000

PLANE	SEGMENT	FORCE DEFLECTION	INERTIAL SPIKE	R FACTOR	G FACTOR	FRICTION COEF. OPT
1- 6	1- 1	8	0	26	0	25 1
GROUND PLANE (FRONT)	CAR FRONT SUSPENSION STI			R FACTOR = 0.80 T		FRICTION = 0.0 (ROLL
1- 6	1- 7	8	0	26	0	25 1
GROUND PLANE (FRONT)	CAR FRONT SUSPENSION STI			R FACTOR = 0.80 T		FRICTION = 0.0 (ROLL
1- 6	1- 8	6	0	26	0	25 1
GROUND PLANE (FRONT)	CAR REAR SUSPENSION STIF			R FACTOR = 0.80 T		FRICTION = 0 0 (ROLL
1- 6	1- 9	6	0	26	0	25 1
GROUND PLANE (FRONT)	CAR REAR SUSPENSION STIF			R FACTOR = 0 80 T		FRICTION = 0.0 (ROLL
2- 6	1- 10	33	-9	-21	-40	36 1
GROUND PLANE (REAR)	CAR CONSTANT = 0.0 (HARD		BODY STIFFNESS	BODY ABSORPTION	BODY VISCOSITY	FRICTION = 0.60
2- 6	1- 11	33	-9	-21	-40	36 1
GROUND PLANE (REAR)	CAR CONSTANT = 0.0 (HARD		BODY STIFFNESS	BODY ABSORPTION	BODY VISCOSITY	FRICTION = 0.60
2- 6	1- 12	33	-9	-21	-40	36 1
GROUND PLANE (REAR)	CAR CONSTANT = 0.0 (HARD		BODY STIFFNESS	BODY ABSORPTION	BODY VISCOSITY	FRICTION = 0.60
2- 6	1- 13	33	-9	-21	-40	36 1
GROUND PLANE (REAR)	CAR CONSTANT = 0.0 (HARD		BODY STIFFNESS	BODY ABSORPTION	BODY VISCOSITY	FRICTION = 0.60
2- 6	1- 14	33	-9	-21	-40	36 1
GROUND PLANE (REAR)	CAR CONSTANT = 0.0 (HARD		BODY STIFFNESS	BODY ABSORPTION	BODY VISCOSITY	FRICTION = 0.60
3- 6	1- 1	33	-10	-20	-40	23 1
RAIL TOP 1 (STRAIGHT	CAR CONSTANT = 0.0 (HARD		GUARDRAIL STIFFNESS	GUARDRAIL ABSORPTIO	BODY VISCOSITY	FRICTION = 0.30
3- 6	1- 7	33	-10	-20	-40	23 1
RAIL TOP 1 (STRAIGHT	CAR CONSTANT = 0.0 (HARD		GUARDRAIL STIFFNESS	GUARDRAIL ABSORPTIO	BODY VISCOSITY	FRICTION = 0.30
3- 6	1- 8	33	-10	-20	-40	23 1
RAIL TOP 1 (STRAIGHT	CAR CONSTANT = 0.0 (HARD		GUARDRAIL STIFFNESS	GUARDRAIL ABSORPTIO	BODY VISCOSITY	FRICTION = 0.30
3- 6	1- 9	33	-10	-20	-40	23 1
RAIL TOP 1 (STRAIGHT	CAR CONSTANT = 0.0 (HARD		GUARDRAIL STIFFNESS	GUARDRAIL ABSORPTIO	BODY VISCOSITY	FRICTION = 0.30
3- 6	1- 10	29	-10	-20	-40	23 1
RAIL TOP 1 (STRAIGHT	CAR	CONSTANT = 0.0 (SO	GUARDRAIL STIFFNESS	GUARDRAIL ABSORPTIO	BODY VISCOSITY	FRICTION = 0.30

```
     4- 6          1- 11     29                  -10              -20                  -40              23          1
RAIL TOP 2 (STRAIGHT  CAR   CONSTANT = 0 0 (SO GUARDRAIL STIFFNESS  GUARDRAIL ABSORPTIO BODY VISCOSITY  FRICTION = 0 30
     4- 6          1- 12     29                  -10              -20                  -40              23          1
RAIL TOP 2 (STRAIGHT  CAR   CONSTANT = 0 0 (SO GUARDRAIL STIFFNESS  GUARDRAIL ABSORPTIO BODY VISCOSITY  FRICTION = 0 30
     4- 6          1- 13     29                  -10              -20                  -40              23          1
RAIL TOP 2 (STRAIGHT  CAR   CONSTANT = 0 0 (SO GUARDRAIL STIFFNESS  GUARDRAIL ABSORPTIO BODY VISCOSITY  FRICTION = 0 30
     4- 6          1- 14     29                  -10              -20                  -40              23          1
RAIL TOP 2 (STRAIGHT  CAR   CONSTANT = 0 0 (SO GUARDRAIL STIFFNESS  GUARDRAIL ABSORPTIO BODY VISCOSITY  FRICTION = 0 30
     5- 6          1- 1      29                   0                0                    0                25          1
RAIL +SIDE 1 (STRAIG  CAR   CONSTANT = 0 0 (SO                                                          FRICTION = 0 0 (ROLL
     5- 6          1- 7      29                   0                0                    0                25          1
RAIL +SIDE 1 (STRAIG  CAR   CONSTANT = 0 0 (SO                                                          FRICTION = 0.0 (ROLL
     5- 6          1- 8      29                   0                0                    0                25          1
RAIL +SIDE 1 (STRAIG  CAR   CONSTANT = 0 0 (SO                                                          FRICTION = 0 0 (ROLL
     5- 6          1- 9      29                   0                0                    0                25          1
RAIL +SIDE 1 (STRAIG  CAR   CONSTANT = 0 0 (SO                                                          FRICTION = 0 0 (ROLL
     5- 6          1- 10     29                   0                0                    0                25          1
RAIL +SIDE 1 (STRAIG  CAR   CONSTANT = 0 0 (SO                                                          FRICTION = 0 0 (ROLL
     6- 6          1- 11     29                   0                0                    0                25          1
RAIL +SIDE 2 (STRAIG  CAR   CONSTANT = 0 0 (SO                                                          FRICTION = 0 0 (ROLL
     6- 6          1- 12     29                   0                0                    0                25          1
RAIL +SIDE 2 (STRAIG  CAR   CONSTANT = 0 0 (SO                                                          FRICTION = 0 0 (ROLL
     6- 6          1- 13     29                   0                0                    0                25          1
RAIL +SIDE 2 (STRAIG  CAR   CONSTANT = 0 0 (SO                                                          FRICTION = 0.0 (ROLL
     6- 6          1- 14     29                   0                0                    0                25          1
RAIL +SIDE 2 (STRAIG  CAR   CONSTANT = 0 0 (SO                                                          FRICTION = 0.0 (ROLL
     7- 6          1- 1      33                  -7               -20                  -40              23          1
RAIL TOP 1 (SLANTED)  CAR CONSTANT = 0 0 (HARD SLANTED GUARDRAIL ST  GUARDRAIL ABSORPTIO BODY VISCOSITY  FRICTION = 0.30
     7- 6          1- 7      33                  -7               -20                  -40              23          1
RAIL TOP 1 (SLANTED)  CAR CONSTANT = 0 0 (HARD SLANTED GUARDRAIL ST  GUARDRAIL ABSORPTIO BODY VISCOSITY  FRICTION = 0 30
     7- 6          1- 8      33                  -7               -20                  -40              23          1
RAIL TOP 1 (SLANTED)  CAR CONSTANT = 0 0 (HARD SLANTED GUARDRAIL ST  GUARDRAIL ABSORPTIO BODY VISCOSITY  FRICTION = 0.30
```

```
     7- 6          1- 9      33                    -7                -20                -40                  23                1
RAIL TOP 1 (SLANTED)  CAR CONSTANT = 0.0 (HARD SLANTED GUARDRAIL ST  GUARDRAIL ABSORPTIO BODY VISCOSITY      FRICTION = 0.30
     7- 6          1- 10     29                    -7                -20                -40                  35                1
RAIL TOP 1 (SLANTED)  CAR   CONSTANT = 0 0 (SO SLANTED GUARDRAIL ST  GUARDRAIL ABSORPTIO BODY VISCOSITY      FRICTION = 0.70
     8- 6          1- 11     29                    -7                -20                -40                  35                1
RAIL TOP 2 (SLANTED)  CAR   CONSTANT = 0 0 (SO SLANTED GUARDRAIL ST  GUARDRAIL ABSORPTIO BODY VISCOSITY      FRICTION = 0.70
     8- 6          1- 12     29                    -7                -20                -40                  35                1
RAIL TOP 2 (SLANTED)  CAR   CONSTANT = 0.0 (SO SLANTED GUARDRAIL ST  GUARDRAIL ABSORPTIO BODY VISCOSITY      FRICTION = 0.70
     8- 6          1- 13     29                    -7                -20                -40                  35                1
RAIL TOP 2 (SLANTED)  CAR   CONSTANT = 0.0 (SO SLANTED GUARDRAIL ST  GUARDRAIL ABSORPTIO BODY VISCOSITY      FRICTION = 0.70
     8- 6          1- 14     29                    -7                -20                -40                  35                1
RAIL TOP 2 (SLANTED)  CAR   CONSTANT = 0.0 (SO SLANTED GUARDRAIL ST  GUARDRAIL ABSORPTIO BODY VISCOSITY      FRICTION = 0.70
     9- 6          1- 1      29                    0                 0                  0                    25                1
RAIL +SIDE 1 (SLANTE  CAR   CONSTANT = 0.0 (SO                                                              FRICTION = 0.0 (ROLL
     9- 6          1- 7      29                    0                 0                  0                    25                1
RAIL +SIDE 1 (SLANTE  CAR   CONSTANT = 0.0 (SO                                                              FRICTION = 0.0 (ROLL
     9- 6          1- 8      29                    0                 0                  0                    25                1
RAIL +SIDE 1 (SLANTE  CAR   CONSTANT = 0.0 (SO                                                              FRICTION = 0.0 (ROLL
     9- 6          1- 9      29                    0                 0                  0                    25                1
RAIL +SIDE 1 (SLANTE  CAR   CONSTANT = 0 0 (SO                                                              FRICTION = 0 0 (ROLL
     9- 6          1- 10     29                    0                 0                  0                    25                1
RAIL +SIDE 1 (SLANTE  CAR   CONSTANT = 0 0 (SO                                                              FRICTION = 0.0 (ROLL
     10- 6         1- 11     29                    0                 0                  0                    25                1
RAIL +SIDE 2 (SLANTE  CAR   CONSTANT = 0.0 (SO                                                              FRICTION = 0.0 (ROLL
     10- 6         1- 12     29                    0                 0                  0                    25                1
RAIL +SIDE 2 (SLANTE  CAR   CONSTANT = 0.0 (SO                                                              FRICTION = 0.0 (ROLL
     10- 6         1- 13     29                    0                 0                  0                    25                1
RAIL +SIDE 2 (SLANTE  CAR   CONSTANT = 0.0 (SO                                                              FRICTION = 0 0 (ROLL
     10- 6         1- 14     29                    0                 0                  0                    25                1
RAIL +SIDE 2 (SLANTE  CAR   CONSTANT = 0.0 (SO                                                              FRICTION = 0.0 (ROLL
     11- 6         1- 1      33                    -8                -34                -40                  24                1
GROUND PLANE (REAR)   CAR CONSTANT = 0.0 (HARD FRONT SUSPENSION STI  TIRE/GRND ABSORPTIO BODY VISCOSITY      FRICTION = 0.80 (TIR
```

```
   11- 6        1- 7     33                    -8              -34                -40              24              1
GROUND PLANE (REAR)  CAR CONSTANT = 0 0 (HARD FRONT SUSPENSION STI  TIRE/GRND ABSORPTIO BODY VISCOSITY  FRICTION = 0 80 (TIR
   11- 6        1- 8     33                    -6              -34                -40              24              1
GROUND PLANE (REAR)  CAR CONSTANT = 0 0 (HARD REAR SUSPENSION STIF  TIRE/GRND ABSORPTIO BODY VISCOSITY  FRICTION = 0 80 (TIR
   11- 6        1- 9     33                    -6              -34                -40              24              1
GROUND PLANE (REAR)  CAR CONSTANT = 0 0 (HARD REAR SUSPENSION STIF  TIRE/GRND ABSORPTIO BODY VISCOSITY  FRICTION = 0.80 (TIR
                                                                                                      CARDS F 3
   SEGMENT      SEGMENT  FORCE DEFLECTION      INERTIAL SPIKE      R FACTOR           G FACTOR        FRICTION COEF  OPT
    2- 2         1- 10     29                    -11             -21                -40              23              0
     PST1         CAR   CONSTANT = 0 0 (SO POST STIFFNESS      BODY ABSORPTION  BODY VISCOSITY  FRICTION = 0 30
    2- 2         1- 11     29                    -11             -21                -40              23              0
     PST1         CAR   CONSTANT = 0 0 (SO POST STIFFNESS      BODY ABSORPTION  BODY VISCOSITY  FRICTION = 0 30
    2- 2         1- 12     29                    -11             -21                -40              23              0
     PST1         CAR   CONSTANT = 0 0 (SO POST STIFFNESS      BODY ABSORPTION  BODY VISCOSITY  FRICTION = 0 30
    2- 2         1- 13     29                    -11             -21                -40              23              0
     PST1         CAR   CONSTANT = 0 0 (SO POST STIFFNESS      BODY ABSORPTION  BODY VISCOSITY  FRICTION = 0 30
    2- 2         1- 14     29                    -11             -21                -40              23              0
     PST1         CAR   CONSTANT = 0 0 (SO POST STIFFNESS      BODY ABSORPTION  BODY VISCOSITY  FRICTION = 0 30
    3- 3         1- 10     29                    -11             -21                -40              23              0
     PST9         CAR   CONSTANT = 0.0 (SO POST STIFFNESS      BODY ABSORPTION  BODY VISCOSITY  FRICTION = 0 30
    3- 3         1- 11     29                    -11             -21                -40              23              0
     PST9         CAR   CONSTANT = 0.0 (SO POST STIFFNESS      BODY ABSORPTION  BODY VISCOSITY  FRICTION = 0 30
    3- 3         1- 12     29                    -11             -21                -40              23              0
     PST9         CAR   CONSTANT = 0 0 (SO POST STIFFNESS      BODY ABSORPTION  BODY VISCOSITY  FRICTION = 0 30
    3- 3         1- 13     29                    -11             -21                -40              23              0
     PST9         CAR   CONSTANT = 0 0 (SO POST STIFFNESS      BODY ABSORPTION  BODY VISCOSITY  FRICTION = 0 30
    3- 3         1- 14     29                    -11             -21                -40              23              0
     PST9         CAR   CONSTANT = 0 0 (SO POST STIFFNESS      BODY ABSORPTION  BODY VISCOSITY  FRICTION = 0 30
    4- 4         1- 10     29                    -11             -21                -40              23              0
     PS10         CAR   CONSTANT = 0 0 (SO POST STIFFNESS      BODY ABSORPTION  BODY VISCOSITY  FRICTION = 0 30
    4- 4         1- 11     29                    -11             -21                -40              23              0
     PS10         CAR   CONSTANT = 0 0 (SO POST STIFFNESS      BODY ABSORPTION  BODY VISCOSITY  FRICTION = 0 30
```

4- 4	1- 12	29			-11	-21		-40	23		0
PS10	CAR	CONSTANT = 0.0 (SO POST STIFFNESS				BODY ABSORPTION		BODY VISCOSITY	FRICTION = 0.30		
4- 4	1- 13	29			-11	-21		-40	23		0
PS10	CAR	CONSTANT = 0.0 (SO POST STIFFNESS				BODY ABSORPTION		BODY VISCOSITY	FRICTION = 0 30		
4- 4	1- 14	29			-11	-21		-40	23		0
PS10	CAR	CONSTANT = 0.0 (SO POST STIFFNESS				BODY ABSORPTION		BODY VISCOSITY	FRICTION = 0.30		

SUBROUTINE INITAL INPUT

CARD G.1

ZPLT(X)	ZPLT(Y)	ZPLT(Z)	I1	J1	I2	J2	I3	SPLT(1)	SPLT(2)	SPLT(3)
0.	0.	0.	0	0	0	0	1	10 00	6 00	1 00

INITIAL POSITIONS (INERTIAL REFERENCE)

CARDS G.2

SEGMENT	LINEAR POSITION (IN.)			LINEAR VELOCITY (IN./SEC.)		
NO. SEG	X	Y	Z	X	Y	Z
1 CAR	0.00000	-2.50000	-20.30000	1056 00000	0.00000	0.00000
2 PST1	261.00000	-23.00000	-14.00000	0.00000	0.00000	0.00000
3 PST9	861.00000	-25.50000	-10.50000	0 00000	0.00000	0.00000
4 PS10	936.00000	-25.50000	-10.50000	0.00000	0.00000	0.00000

INITIAL ANGULAR ROTATION AND VELOCITY

CARDS G.3

SEGMENT	ANGULAR ROTATION (DEG)			ANGULAR VELOCITY (DEG/SEC.)						
NO. SEG	YAW	PITCH	ROLL	X	Y	Z	IYPR			
1 CAR	0.00000	0.00000	0.00000	0.00000	0.00000	0.00000	3	2	1	0
2 PST1	0.00000	0.00000	0.00000	0.00000	0.00000	0.00000	3	2	1	0
3 PST9	0.00000	0.00000	0.00000	0.00000	0.00000	0.00000	3	2	1	0
4 PS10	0 00000	0.00000	0.00000	0.00000	0.00000	0.00000	3	2	1	0

TABULAR TIME HISTORY CONTROL PARAMETERS

TYPE	KSG	SELECTED SEGMENTS OR JOINTS
H 1	1	1
REF		6
H 2	1	1
REF		6
H 3	1	1
REF		6
H 4	1	1
REF		1
H.5	1	1
REF		1
H 6	1	1
REF		6
H 7	0	
REF		
H 8	0	
REF		
H 9	0	
REF		
H.10	1	1
REF		6

MAIN3D FUNCTIONS FOR TIME= 0.000 MSEC

SEGMENT	(INERTIAL) ANGULAR ROTATION (DEG) YAW	PITCH	ROLL	(LOCAL) ANGULAR VELOCITY (RAD/SEC.) X	Y	Z	(LOCAL) ANGULAR ACCELERATION (RAD/SEC.**2) X	Y	Z
1 CAR	0.0000	0.0000	0.0000	0.00000	0 00000	0.00000	2.541318	0 719863	-0 158483
2 PST1	0.0000	0.0000	0.0000	0.00000	0.00000	0 00000	0.000000	0.000000	0 000000
3 PST9	0.0000	0.0000	0.0000	0.00000	0.00000	0.00000	0.000000	0.000000	0 000000
4 PS10	0.0000	0.0000	0.0000	0 00000	0.00000	0.00000	0.000000	0.000000	0 000000
5 VEH	0.0000	0.0000	0.0000	0.00000	0.00000	0.00000	0.000000	0.000000	0 000000

SEGMENT	(INERTIAL) LINEAR POSITION (IN.) X	Y	Z	(INERTIAL) LINEAR VELOCITY (IN./SEC.) X	Y	Z	(INERTIAL) LINEAR ACCELERATIONS (G'S) X	Y	Z
1 CAR	0.0000	-2.5000	-20.3000	1056 00000	0.00000	0.00000	-0.055346	0.000000	-0.138913
2 PST1	261.0000	-23.0000	-14 0000	0 00000	0.00000	0.00000	0.000000	0.000000	0 000000
3 PST9	861.0000	-25.5000	-10 5000	0 00000	0.00000	0.00000	0.000000	0.000000	0.000000
4 PS10	936.0000	-25.5000	-10.5000	0 00000	0.00000	0.00000	0.000000	0.000000	0.000000
5 VEH	0.0000	0.0000	0 0000	0 00000	0.00000	0.00000	0 000000	0.000000	0.000000

SEGMENT	(INERTIAL) U1 ARRAY (IN./SEC.**2) EXTERNAL LINEAR ACCELERATIONS X	Y	Z	(LOCAL) U2 ARRAY (RAD/SEC.**2) EXTERNAL ANGULAR ACCELERATIONS X	Y	Z	KINETIC ENERGY (LB.- IN) LINEAR	ANGULAR	TOTAL
1 CAR	-0.2137D+02	0.0000D+00	-0.5363D+02	0.25413D+01	0.71986D+00	-0.15848D+00	0.40612D+07	0.00000D+00	0 40612D+07
2 PST1	0.0000D+00	0.0000D+00	0.0000D+00	0.00000D+00	0.00000D+00	0 00000D+00	0.00000D+00	0.00000D+00	0 00000D+00
3 PST9	0.0000D+00	0.0000D+00	0.0000D+00	0.00000D+00	0.00000D+00	0.00000D+00	0.00000D+00	0.00000D+00	0.00000D+00
4 PS10	0.0000D+00	0.0000D+00	0.0000D+00	0.00000D+00	0.00000D+00	0.00000D+00	0.00000D+00	0.00000D+00	0.00000D+00

REFERENCES

1. Fleck, J.T., Butler, F.E. and DeLeys, N.J., "Validation of the Crash Victim Simulator," Report Nos. DOT-HS-806-279 thru 282, 1982, Vols. 1-4.

2. Butler, F.E. and Fleck, J.T., "Development of an Improved Computer Model of the Human Body and Extremity Dynamics," AMRL-TR-75-14, 1975.

3. Kaleps, I., Obergefell, L.A. and Ryerson, J.R., "Simulation of Restrained Occupant Dynamics During Vehicle Rollover," Report No. DOT-HS-807-049, June 1986.

4. Obergefell, L.A., Rizer, A.L. and Kaleps, I., "Simulations of Rollover Tests," Final Report for DOT Interagency Agreement DTNH22-85-X-07233, May 1988.

5. Obergefell, L.A., Kaleps, I. and Johnson, A.K., "Prediction of an Occupant's Motion During Rollover Crashes," Proc. 30th Stapp Car Crash Conference, SAE Paper No. 861876, October 1986.

6. Segal, D. and Kamholz, L., "Development of a General Rollover Test Device," DOT Report No. HS-806-550, Sept. 1983.

7. Stultz, J.C., "Dummy Kinematics in Controlled Rollover Crashes," Transportation Research Center of Ohio, Report No. TRC-85-NO2, June 1985.

8. "Motor Vehicle Manufacturers Association Specifications Form on the 1981 Dodge Aries," June 1980.

9. Fancher, P.S., et. al., "Limit Handling Performance as Influenced By Degradation of Steering and Suspension Systems," DOT Report No. UM-HSRI-PF-72-3-1, November 1972.

10. Leetch, B.D. and Bowman, W.L., "Articulated Total Body (ATB) VIEW Program Software Report," Report No. AFAMRL-TR-81-111, Vols. 1 and 2, June 1983.

11. Bronstad, M.E. and Mayer, Jr, J.B., "Vehicle Rollover Test RO-2," Southwest Research Institute Test Report on National Highway Traffic Safety Administration Contract No. DTFH61-81-C00076, April 1984.